Electronic Journal of Differential Equations, Vol. 2026 (2026), No. 45, pp. 1–28.
ISSN: 1072-6691. URL: https://ejde.math.txstate.edu, DOI: 10.58997/ejde.2026.45

SPATIOTEMPORAL DYNAMICS AND OPTIMAL CONTROL OF AN INFECTION-AGE STRUCTURED REACTION-DIFFUSION EPIDEMIC MODEL WITH WANING IMMUNITY

NIKHIL CHANAURIA, SYED ABBAS

Abstract. Classical infectious disease models often neglect the interplay of spatial diffusion, infection-age structure, and time-dependent controls. We address this gap by analyzing a spatiotemporal SIQRV reaction-diffusion model structured by infection age, incorporating vaccination, quarantine, and waning immunity. The simultaneous inclusion of nonlocal infection-age structure, spatial diffusion, and time-dependent controls introduces major analytical challenges, including coupled transport-diffusion dynamics, nonlinear nonlocal incidence, and the derivation of optimality conditions in infinite-dimensional spaces. Using semigroup theory and spectral methods, we establish well-posedness, derive the basic reproduction number $\mathcal{R}_0$, and analyze equilibrium stability. An optimal control framework is introduced with vaccination, social distancing, and quarantine as time-varying interventions. Necessary conditions are derived via an adjoint system and solved using a forward-backward sweep method. Simulations with measles-like parameters show that spatially targeted, age-structured interventions effectively suppress outbreaks and improve resource allocation. This study underscores the importance of integrating spatial and temporal heterogeneities in epidemic control strategies.

1. Introduction

Mathematical modeling of infectious diseases has played a foundational role in understanding disease spread and informing public health responses. Classical models, notably the SIR and SEIR frameworks introduced by Kermack and McKendrick [16] and formalized by Hethcote [9], divide the population into compartments and describe transitions between them via systems of ordinary differential equations (ODEs). For instance, the basic SIR model is given by:

$$\begin{aligned} \frac{dS}{dt} &= -\lambda(t) - \mu S, \\ \frac{dI}{dt} &= \lambda(t) - (\rho + \mu) I, \\ \frac{dR}{dt} &= \rho I - \mu R, \end{aligned} \tag{1.1}$$

where $\lambda(t) = \alpha S(t) I(t)$ represents the force of infection. Here α, ρ, and μ are the transmission rate, recovery rate, and mortality rate, respectively. While effective for providing qualitative insights, such models rely on simplifying assumptions, including homogeneous mixing, exponential waiting times, and instantaneous transitions. These limitations can lead to oversimplified dynamics that overlook important biological and epidemiological heterogeneities.

To capture more realistic disease dynamics, researchers have introduced infection-age structured models, where each infected individual is tracked according to the duration of their infection, with τ denoting the infection age. Infection-age models are typically formulated as integro-differential equations or partial differential equations (PDEs) and have been successfully applied to diseases

2020 *Mathematics Subject Classification.* 35F50, 35K57, 92D30.
Key words and phrases. Infection-age structured; reaction-diffusion; stability analysis; optimal control.

Submitted May 5, 2026. Published June 29, 2026.

with pronounced latency or staged infectivity patterns. In this framework, the total infectious load at a time t is given by:

$$I_{\text{tot}}(t) = \int_0^{\tau^+} I(t,\tau)\, d\tau.$$

The density function $I(t,\tau)$ satisfies a transport equation

$$\partial_\tau I(t,\tau) + \partial_t I(t,\tau) = -\mu(\tau) I(t,\tau), \quad I(t,0) = \lambda(t), \tag{1.2}$$

where $\lambda(t)$ is the inflow of new infections at time t and $\mu(\tau)$ is the infection-age dependent removal rate. This approach enables more realistic modeling of disease progression, including incubation periods, variable infectiousness, and delayed recovery or quarantine. Diekmann et al. [7], Inaba [11], and Magal and Ruan [22] have established rigorous formulations and threshold conditions for such models.

Parallel to infection-age models, spatial heterogeneity has been addressed through reaction-diffusion systems, where individual movement is modeled via diffusion. A prototypical spatial SIR model takes the form

$$\begin{aligned}
\frac{\partial S}{\partial t}(t,\rho) &= D_S \Delta S(t,\rho) - \lambda(t) - \mu S(t,\rho),\\
\frac{\partial I}{\partial t}(t,\rho) &= D_I \Delta I(t,\rho) + \lambda(t) - (\gamma+\mu) I(t,\rho),\\
\frac{\partial R}{\partial t}(t,\rho) &= D_R \Delta R(t,\rho) + \gamma I(t,\rho) - \mu R(t,\rho),
\end{aligned} \tag{1.3}$$

with diffusion coefficients D_S, D_I, D_R, and where Δ denotes the Laplace operator. Also, $\rho \in \Omega \subset \mathbb{R}^n$ is a bounded spatial domain. Works by Murray [25], Allen et al. [1], and Zhao et al. [32] have explored traveling wave solutions, spreading speeds, and spatial control in such models. Reaction-diffusion epidemic models have provided valuable tools for understanding the geographic spread of infectious diseases and the role of mobility and spatial structure in controlling outbreaks.

More advanced models combine infection-age structure and spatial diffusion, leading to PDE systems of the form

$$\partial_\tau I(t,\tau,\rho) + \partial_t I(t,\tau,\rho) = D_I \Delta I(t,\tau,\rho) - \mu(\tau) I(t,\tau,\rho), \tag{1.4}$$

$$I(t,0,\rho) = S(t,\rho) \int_0^{\tau^+} k(\tau) i(t,\tau,\rho)\, d\tau, \tag{1.5}$$

where $k(\tau)$ is the infection-age dependent transmission rate. Also, the Neumann boundary conditions are typically imposed. Walker [27] and Wu et al. [30] have analyzed such systems using semigroup theory and established well-posedness and long-time behavior.

Recent studies have demonstrated the rich dynamics that emerge when spatial diffusion interacts with nonlinear infection processes. For example, Lei et al. [17] studied the asymptotic behavior of a reaction-diffusion SEIR epidemic model in a heterogeneous environment. Meng and Zhu [23] studied the effect of vaccination and quarantine strategies on disease transmission of an SIER model with a nonlinear incidence rate. Zhao et al. [33] investigated the optimal control of a diffusive SVIR model. Walker [27] established the principle of linearized stability and instability for a classical model describing the spatial movement of an age-structured population. Wu et al. [30] established the existence of both supercritical and critical traveling waves. Beyond epidemic models, related analytical questions concerning global well-posedness, boundedness, stability, and spatiotemporal dynamics have also been extensively investigated in Keller-Segel type chemotaxis systems. In particular, the recent works [14, 19] analyzes the role of dissipative gradient nonlinearities in preventing concentration phenomena in local and nonlocal attraction-repulsion chemotaxis models, providing further insight into the analysis of nonlinear spatiotemporal PDE systems. For more literature on such models, we refer to [5, 20, 29, 31].

Although infection-age structure, spatial diffusion, and optimal control have each been studied extensively, their integration within a unified modeling framework remains limited. This represents a notable gap in epidemic modeling, particularly for diseases where both temporal and spatial

heterogeneities significantly influence transmission dynamics. Bridging this gap offers both mathematical depth and practical relevance for designing targeted, spatially informed interventions. Motivated by these considerations, we propose and analyze a spatiotemporal partial differential equation (PDE) model incorporating infection-age structure and spatial diffusion across five epidemiological compartments: Susceptible (S), Infected (I), Quarantined (Q), Recovered (R), and Vaccinated (V). The infected class is structured by infection age, allowing temporally resolved infectivity and progression. Spatial diffusion is modeled via Laplacian operators acting on mobile compartments within a bounded domain under homogeneous Neumann (no-flux) boundary conditions. The model incorporates quarantine measures to isolate infected individuals and vaccination strategies targeting both susceptible and recovered individuals, accounting for preventive protection and waning immunity.

The proposed model presents significant analytical challenges due to its integration of infection-age structure, spatial diffusion, and time-dependent control. The nonlocal and nonlinear force of infection, involving an integral over infection age, complicates standard analysis and requires careful functional setup. The infected population evolves according to a transport-diffusion equation in both age and space, combining hyperbolic and parabolic features. To handle this, we apply the method of characteristics in the infection-age direction and semigroup theory for diffusion operators. The age-dependent quarantine and recovery terms introduce variable coefficients, demanding additional continuity assumptions. Optimal control further complicates the problem, yielding a PDE-constrained optimization problem.

This modeling framework is sufficiently general to apply to a wide class of infectious diseases, including those with well-defined latent periods and spatial transmission characteristics. As a representative example, we mention measles [21, 24], a highly contagious viral disease that has been extensively modeled in both age-structured and spatial settings. Measles features a latency period of 7-18 days, followed by a prodrome stage of 2-4 days marked by early symptoms such as fever, cough, and conjunctivitis, with increasing infectivity. The rash phase, typically occurring between days 14 and 21 post-infection, corresponds to peak infectivity, making measles well-suited to infection-age structured modeling. Furthermore, its potential for rapid spatial spread and the role of quarantine and vaccination in its control provide additional motivation for the type of model studied in this work. Recent studies [12, 15] have examined measles transmission dynamics under incomplete vaccination, resurgence in spatially heterogeneous populations, and the effects of delayed immunity and spatial mobility. These investigations underscore the need for models that integrate both temporal and spatial heterogeneities, particularly when assessing intervention strategies. However, the theoretical and numerical results we present are not restricted to measles only and may be applied to a broad class of diseases with similar biological properties.

The paper is structured as follows. In Section 2, we formulate our model by first highlighting all the assumptions required to describe the model structure. In Section 3, we prove the well-posedness results for our model. Section 4 is devoted to the analysis of the model, including the derivation of the basic reproduction number and equilibrium properties. Section 5 introduces the optimal control problem and derives the necessary conditions for optimality. Section 6 presents the numerical implementation and simulation results. We conclude in Section 7 with a discussion of implications, limitations, and possible extensions.

2. Model formulation

Let $S(t,\rho), Q(t,\rho), R(t,\rho)$, and $V(t,\rho)$ represent the population densities of susceptible, quarantined, recovered, and vaccinated individuals, respectively, at time $t \geq 0$ and at location $\rho \in \Omega$. $\Omega \subseteq \mathbb{R}^N$ is a bounded spatial domain. The infected population density with infection age $\tau \in [0, \tau^+]$ is denoted by $I(t,\tau,\rho)$, where $t \geq 0$ represents time and $\rho \in \Omega$. The parameter τ^+ represents the maximum possible duration of infection, which can be either finite or infinite.

Considering real-life scenarios, we imposed the following key assumptions:

(1) Only infected individuals are quarantined, as they pose the highest risk of transmitting the disease. Quarantining other individuals who are not yet infectious may be unnecessary or inefficient, given the potential for false positives and the associated social and economic

burdens. Instead, focusing quarantine efforts on actively infectious individuals helps optimize containment strategies while minimizing disruptions to the broader population.

(2) Vaccination is administered exclusively to susceptible and recovered individuals. This assumption ensures that only those who have never been infected or have already overcome the infection receive immunity, preventing unnecessary vaccination of individuals who are currently infected or quarantined. Moreover, prioritizing these groups helps in curbing disease transmission while reinforcing immunity within the population.

(3) Recovered individuals can still enter into the susceptible compartment: A case of waning immunity.

While it is always possible to find scenarios where one or more assumptions may not hold, making certain assumptions is essential for deriving meaningful results. Given these foundational assumptions, the evolution of the disease across temporal, spatial, and infection-age dimensions is described by the following set of partial differential equations

$$\begin{aligned}
\frac{\partial S(t,\rho)}{\partial t} &= A + d_S\Delta S(t,\rho) - (\mu+v_S)S(t,\rho) - \frac{S(t,\rho)}{N}\int_0^{\tau^+}\beta(\tau)I(t,\tau,\rho)\,d\tau + \delta R(t,\rho),\\
\frac{\partial I(t,\tau,\rho)}{\partial \tau} + \frac{\partial I(t,\tau,\rho)}{\partial t} &= d_I\Delta I(t,\tau,\rho) - (\mu + q_I(\tau) + \sigma_I(\tau) + d(\tau))I(t,\tau,\rho),\\
\frac{\partial Q(t,\rho)}{\partial t} &= d_Q\Delta Q(t,\rho) - (\sigma_Q+\mu)Q(t,\rho) + \int_0^{\tau^+} q_I(\tau)I(t,\tau,\rho)\,d\tau,\\
\frac{\partial R(t,\rho)}{\partial t} &= d_R\Delta R(t,\rho) - (v_R+\delta+\mu)R(t,\rho) + \int_0^{\tau^+}\sigma_I(\tau)I(t,\tau,\rho)\,d\tau + \sigma_Q Q(t,\rho),\\
\frac{\partial V(t,\rho)}{\partial t} &= d_V\Delta V(t,\rho) + v_R R(t,\rho) + v_S S(t,\rho) - \mu V(t,\rho),\\
I(t,0,\rho) &= \frac{S(t,\rho)}{N}\int_0^{\tau^+}\beta(\tau)I(t,\tau,\rho)\,d\tau, \quad t\geq 0,\ \rho\in\Omega,\\
\frac{\partial S(t,\rho)}{\partial n} &= \frac{\partial I(t,\tau,\rho)}{\partial n} = \frac{\partial Q(t,\rho)}{\partial n} = \frac{\partial R(t,\rho)}{\partial n} = \frac{\partial V(t,\rho)}{\partial n} = 0, \quad \rho\in\mathbb{R}^N\setminus\Omega,\\
S(0,\rho) &= S_0(\rho), \quad I(0,\tau,\rho) = I_0(\tau,\rho), \quad Q(0,\rho) = Q_0(\rho),\\
R(0,\rho) &= R_0(\rho), \quad V(0,\rho) = V_0(\rho).
\end{aligned} \tag{2.1}$$

The parameter $A \geq 0$ represents the rate at which susceptible individuals enter the population. Constants $d_S, d_I, d_Q, d_R(\geq 0)$ and $d_V \geq 0$ correspond to the diffusion rate of susceptible, infected, quarantined, recovered, and vaccinated individuals, respectively, capturing how each group moves within the spatial domain. The function $\beta(\tau)$ denotes the transmission rate, which depends on the time $\tau \geq 0$ since an individual became infected. The natural mortality rate is given by $\mu \geq 0$, while $d(\tau)$ represents the infection-age dependent disease-induced mortality rate. $\delta \geq 0$ governs the rate at which recovered individuals lose immunity and re-enter the susceptible class. The vaccination rates for susceptible and recovered individuals are denoted by $v_S \geq 0$ and $v_R \geq 0$, respectively. Recovery dynamics of quarantined individuals is characterized by $\sigma_Q \geq 0$, while $\sigma_I(\tau)$ accounts for the recovery rate of infected individuals. Finally, $q_I(\tau)$ describes the rate at which infected individuals are quarantined.

Remark 2.1. The structure of the proposed model is chosen to reflect how infectious diseases evolve in real populations, while remaining amenable to rigorous analysis. The infection-age variable allows key epidemiological processes, such as transmission, quarantine, and recovery, to depend on the stage of infection. This is particularly important for acute diseases, where individuals are not equally infectious throughout the course of illness. By including infection age explicitly, the model can distinguish early, highly infectious stages from later stages with reduced transmission, a feature that cannot be captured by classical compartmental models.

To ensure the biological plausibility of the model, we adopt the following assumptions on the model parameters.

Assumption 2.2. The functions $d, \beta, \sigma_I, q_I \in L^\infty_+(0,\tau^+)$ and let

$$\sigma_I^M = \sup_{\tau\in(0,\tau^+)} \sigma_I(\tau), \quad q_I^M = \sup_{\tau\in(0,\tau^+)} q_I(\tau), \quad \beta^M = \sup_{\tau\in(0,\tau^+)} \beta(\tau), \quad d^M = \sup_{\tau\in(0,\tau^+)} d(\tau).$$

We also introduce an additional assumption, which will prove useful in analyzing the local asymptotic stability of equilibrium points.

Assumption 2.3. The maximum values σ_I^M and q_I^M satisfy

$$(\sigma_I^M + q_I^M)\tau^+ < 1.$$

This assumption ensures that, on average, an infected individual does not recover or get quarantined too quickly over the entire infection-age interval $[0,\tau^+]$.

Remark 2.4. Biologically, the Assumption 2.3 ensures that a positive fraction of infected individuals remain infectious until age τ^+, which is necessary for sustained transmission. Mathematically, this assumption is crucial in the analysis of the local asymptotic stability of equilibrium points, as it guarantees that the total outflow from the infected class does not dominate the system dynamics, thereby preventing premature clearance of infection and ensuring the validity of linearization techniques around equilibria. It also ensures that certain integral terms in the characteristic equation do not dominate and destabilize the system.

3. Well posedness

First of all, we define the functional space. Let $\mathbb{X} = C(\overline{\Omega},\mathbb{R})$, where for any $\phi\in\mathbb{X}$ its norm is defined by

$$\|\phi\|_{\mathbb{X}} = \sup_{\rho\in\overline{\Omega}} |\phi(\rho)|,$$

and $\mathbb{Y} = L^2((0,\tau^+),\mathbb{X})$, where for any $\psi\in\mathbb{Y}$ its norm is defined by

$$\|\psi\|_{\mathbb{Y}} = \Big(\int_0^{\tau^+} \Big(\sup_{\rho\in\overline{\Omega}} |\psi(\tau,\rho)|\Big)^2 d\tau\Big)^{1/2}.$$

Let $\mathbb{Y}_+ = \{\phi\in\mathbb{Y} : \phi\geq 0\}$ and $\mathbb{X}_+ = \{\psi\in\mathbb{X} : \psi\geq 0\}$ denote the positive cones of space $\mathbb{Y}$ and $\mathbb{X}$, respectively.

Let $a_S = v_S + \mu$, $a_I = \mu$, $a_Q = \sigma_Q + \mu$ and $a_R = v_R + \delta + \mu$. From system (2.1), note that the equation concerning vaccinated individuals is decoupled from the other four equations. As a result, excluding this equation does not interfere with the overall analysis. So the model now becomes

$$\begin{aligned}
\frac{\partial S(t,\rho)}{\partial t} &= A + d_S\Delta S(t,\rho) - \frac{S(t,\rho)}{N}\int_0^{\tau^+} \beta(\tau)I(t,\tau,\rho)\,d\tau + \delta R(t,\rho) - a_S S(t,\rho),\\
\frac{\partial I(t,\tau,\rho)}{\partial \tau} + \frac{\partial I(t,\tau,\rho)}{\partial t} &= d_I\Delta I(t,\tau,\rho) - (a_I + q_I(\tau) + \sigma_I(\tau) + d(\tau))I(t,\tau,\rho),\\
\frac{\partial Q(t,\rho)}{\partial t} &= d_Q\Delta Q(t,\rho) - a_Q Q(t,\rho) + \int_0^{\tau^+} q_I(\tau)I(t,\tau,\rho)\,d\tau,\\
\frac{\partial R(t,\rho)}{\partial t} &= d_R\Delta R(t,\rho) - a_R R(t,\rho) + \int_0^{\tau^+} \sigma_I(\tau)I(t,\tau,\rho)d\tau + \sigma_Q Q(t,\rho),\\
I(t,0,\rho) &= \frac{S(t,\rho)}{N}\int_0^{\tau^+} \beta(\tau)I(t,\tau,\rho)\,d\tau, \quad t\geq 0,\ \rho\in\Omega,\\
\frac{\partial S(t,\rho)}{\partial n} &= \frac{\partial I(t,\tau,\rho)}{\partial n} = \frac{\partial Q(t,\rho)}{\partial n} = \frac{\partial R(t,\rho)}{\partial n} = 0, \quad \rho\in\mathbb{R}^N\setminus\Omega,\\
S(0,\rho) &= S_0(\rho), \quad I(0,\tau,\rho) = I_0(\tau,\rho), \quad Q(0,\rho) = Q_0(\rho), \quad R(0,\rho) = R_0(\rho).
\end{aligned} \tag{3.1}$$

Note that from [26], the operators $d_S\Delta S - a_S S$, $d_I\Delta I - a_I I$, $d_Q\Delta Q - a_Q Q$ and $d_R\Delta R - a_R R$ with Neumann boundary condition generate C_0-semigroups $T_S(t)$, $T_I(t)$, $T_Q(t)$ and $T_R(t)$, respectively.

We have

$$\begin{aligned}(T_S(t)[\psi_1])(\rho) &= e^{-a_S t}\int_\Omega G_S(t,\rho,y)\psi_1(y)dy,\\ (T_I(t)[\psi_2])(\tau,\rho) &= e^{-a_I t}\int_\Omega G_I(t,\rho,y)\psi_2(\tau,y)dy,\\ (T_Q(t)[\psi_3])(\rho) &= e^{-a_Q t}\int_\Omega G_Q(t,\rho,y)\psi_3(y)dy,\\ (T_R(t)[\psi_4])(\rho) &= e^{-a_R t}\int_\Omega G_R(t,\rho,y)\psi_4(y)dy,\end{aligned} \tag{3.2}$$

where $\psi=(\psi_1,\psi_2,\psi_3,\psi_4)\in \mathbb{X}\times\mathbb{Y}\times\mathbb{X}\times\mathbb{X}$ and $G_i(i=S,I,Q,R)$ denote the Green functions that are the fundamental solution of the operator $d_i\Delta(\cdot)(i=S,I,Q,R)$, respectively with Neumann boundary condition. Also,

$$\int_\Omega G_i(t,z,y)dy=1,\quad \forall t\geq 0\ (i=S,I,Q,R). \tag{3.3}$$

Let T^* be an arbitrary positive constant. For $(t,\rho)\in(0,T^*)\times\Omega$, define $M_0(t,\rho)=I(t,0,\rho)$. Also for some $k\in\mathbb{R}$, define $M_k(t,\rho)=I(t,t+k,\rho)$, then

$$\frac{\partial M_k(t,\rho)}{\partial t}=\frac{\partial I(t,t+k,\rho)}{\partial t}+\frac{\partial I(t,t+k,\rho)}{\partial \tau}.$$

Setting $t_k=\max\{0,-k\}$, we obtain partial differential equations for the infection density concerning infection age τ by

$$\begin{aligned}\frac{\partial M_k(t,\rho)}{\partial t} &= d_I\Delta M_k(t,\rho)-\mu M_k(t,\rho)-m(t+k)M_k(t,\rho), \quad t\geq t_k,\ \rho\in\Omega,\\ \frac{\partial M_k(t,\rho)}{\partial n} &= 0, \qquad\qquad\qquad\qquad\qquad\qquad\qquad\qquad t\geq t_k,\ \rho\in\mathbb{R}^N\setminus\Omega,\end{aligned} \tag{3.4}$$

where $m(\cdot)=\sigma_I(\cdot)+q_I(\cdot)+d(\cdot)$. Based on equation (3.2), the solution to (3.4) can be expressed as

$$M_k(t,\rho)=e^{-(a_I t+\int_{t_k}^t m(\sigma+k)d\sigma)}\int_\Omega G_I(t-t_k,\rho,y)M_k(t_k,y)dy.$$

Case 1: If $k=\tau-t\geq 0$, then $t_k=0$. Hence for all $\tau\geq t$ we obtain

$$\begin{aligned}I(t,\tau,\rho) &= e^{-(a_I t+\int_0^t m(\sigma+\tau-t)d\sigma)}\int_\Omega G_I(t,\rho,y)M_k(0,y)dy\\ &= e^{-(a_I t+\int_{\tau-t}^\tau m(\sigma)d\sigma)}\int_\Omega G_I(t,\rho,y)I(0,\tau-t,y)dy\\ &= \frac{\Pi(\tau)}{\Pi(\tau-t)}e^{-a_I t}\int_\Omega G_I(t,\rho,y)I_0(\tau-t,y)dy,\end{aligned}$$

where $\Pi(\tau)=e^{-\int_0^\tau m(\sigma)d\sigma}$.

Case 2: If $k=\tau-t<0$, then $t_k=-k=t-\tau$. Hence for all $\tau<t$ we obtain

$$\begin{aligned}I(t,\tau,\rho) &= e^{-(a_I t+\int_{t-\tau}^t m(\sigma+\tau-t)d\sigma)}\int_\Omega G_I(\tau,\rho,y)M_k(t-\tau,y)dy\\ &= e^{-(a_I t+\int_0^\tau m(\sigma)d\sigma)}\int_\Omega G_I(\tau,\rho,y)I(t-\tau,0,y)dy\\ &= \Pi(\tau)e^{-a_I t}\int_\Omega G_I(\tau,\rho,y)M_0(t-\tau,y)dy.\end{aligned}$$

Hence, the solution of the second equation in (3.1) is given by

$$I(t,\tau,\rho)=\begin{cases}\Pi(\tau)e^{-a_I t}\int_\Omega G_I(\tau,\rho,y)M_0(t-\tau,y)dy, & \tau<t,\rho\in\Omega,\\ \frac{\Pi(\tau)}{\Pi(\tau-t)}e^{-a_I t}\int_\Omega G_I(t,\rho,y)I_0(\tau-t,y)dy, & \tau\geq t,\rho\in\Omega.\end{cases} \tag{3.5}$$

Next, we solve (3.1) for the remaining state variables by presenting the following theorem.

Theorem 3.1. *Let initial state of system* (3.1) *be* $(S_0(\rho), I_0(\tau,\rho), Q_0(\rho), R_0(\rho)) \in \mathbb{X}_+ \times \mathbb{Y}_+ \times \mathbb{X}_+ \times \mathbb{X}_+$. *Then, system* (3.1) *admits a unique local mild solution, i.e., there exists* $T > 0$ *such that*

$$(S, I, Q, R) \in C([0,T]; \mathbb{X} \times \mathbb{Y} \times \mathbb{X} \times \mathbb{X}),$$

with I *given by* (3.5).

Proof. First, note that $M_0(t,\rho) = I(t,0,\rho) = \frac{S(t,\rho)}{N} \int_0^{\tau^+} \beta(\tau) I(t,\tau,\rho)\, d\tau$. Now writing the first equation of (3.1) as

$$\frac{\partial S(t,\rho)}{\partial t} = d_S \Delta S(t,\rho) - a_S S(t,\rho) + F(t,\rho),$$

where $F(t,\rho) = A - M_0(t,\rho) + \delta R(t,\rho)$. The solution of this equation takes the form

$$S(t,\rho) = S_1(t,\rho) + \int_0^t e^{-a_S(t-\sigma)} \int_\Omega G_S(t-\sigma,\rho,y)(A - M_0(\sigma,y) + \delta R(\sigma,y))\, dy\, d\sigma, \tag{3.6}$$

where $S_1(t,\rho) = e^{-a_S t} \int_\Omega G_S(t,\rho,y) S_0(y) dy$. Now consider

$$\frac{\partial Q(t,\rho)}{\partial t} = d_Q \Delta Q(t,\rho) - a_Q Q(t,\rho) + \int_0^{\tau^+} q_I(\tau) I(t,\tau,\rho)\, d\tau.$$

The corresponding solution can be written as

$$Q(t,\rho) = Q_1(t,\rho) + \int_0^t e^{-a_Q(t-\sigma)} \int_\Omega G_Q(t-\sigma,\rho,y) Q_2(\sigma,y)\, dy\, d\sigma, \tag{3.7}$$

where $Q_1(t,\rho) = e^{-a_Q t} \int_\Omega G_Q(t,\rho,y) Q_0(y) dy$ and

$$\begin{aligned} Q_2(t,\rho) &= e^{-a_I t} \int_0^t q_I(\tau)\Pi(\tau) \int_\Omega G_I(\tau,\rho,y) M_0(t-\tau,y)\, dy\, d\tau \\ &\quad + e^{-a_I t} \int_t^{\tau^+} q_I(\tau) \frac{\Pi(\tau)}{\Pi(\tau - t)} \int_\Omega G_I(t,\rho,y) I_0(\tau - t, y)\, dy\, d\tau. \end{aligned}$$

Next, we solve the equation

$$\frac{\partial R(t,\rho)}{\partial t} = d_R \Delta R(t,\rho) - a_R R(t,\rho) + \int_0^{\tau^+} \sigma_I(\tau) I(t,\tau,\rho)\, d\tau + \sigma_Q Q(t,\rho).$$

We can write its solution as

$$R(t,\rho) = R_1(t,\rho) + \int_0^t e^{-a_R(t-\sigma)} \int_\Omega G_R(t-\sigma,\rho,y)(R_2(\sigma,y) + \sigma_Q Q(\sigma,y))\, dy\, d\sigma, \tag{3.8}$$

where $R_1(t,\rho) = e^{-a_R t} \int_\Omega G_R(t,\rho,y) R_0(y) dy$ and

$$\begin{aligned} R_2(t,\rho) &= e^{-a_I t} \int_0^t \sigma_I(\tau)\Pi(\tau) \int_\Omega G_I(\tau,\rho,y) M_0(t-\tau,y)\, dy\, d\tau \\ &\quad + e^{-a_I t} \int_t^{\tau^+} \sigma_I(\tau) \frac{\Pi(\tau)}{\Pi(\tau - t)} \int_\Omega G_I(t,\rho,y) I_0(\tau - t, y)\, dy\, d\tau. \end{aligned}$$

Finally, using the definition of $M_0(t,\rho)$, we obtain

$$M_0(t,\rho) = \frac{1}{N}\Big(S_1(t,\rho) + \int_0^t e^{-a_S(t-\sigma)} \int_\Omega G_S(t-\sigma,\rho,y) F(\sigma,y)\, dy\, d\sigma\Big)\Big(\int_0^{\tau^+} \beta(\tau) I(t,\tau,\rho)\, d\tau\Big).$$

Putting all the values we obtain

$$M_0 = \frac{1}{N}\Big(S_1 + L_1(M_0) + L_2(M_0) + L_3(M_0) + K_1\Big)\Big(K_2 + L_4(M_0)\Big), \tag{3.9}$$

where for any $(t,\rho) \in (0,T^*) \times \Omega$,

$$L_1(M_0) = \int_0^t e^{-a_S(t-\sigma)} \int_\Omega G_S(t-\sigma,\rho,y)[A - M_0(\sigma,y)]\, dy\, d\sigma,$$

$$L_2(M_0) = \delta \int_0^t e^{-a_S(t-\sigma)} \int_\Omega G_S(t-\sigma,\rho,y) \int_0^\sigma e^{-a_R(\sigma-s)} \int_\Omega G_R(\sigma-s,y,z) \times \Big[e^{-a_I s} \int_0^s \sigma_I(\tau)\pi(\tau) \int_\Omega G_I(\tau,z,x) M_0(s-\tau,x) dx d\tau\Big] dz\, ds\, dy\, d\sigma,$$

$$L_3(M_0) = \sigma_Q \delta \int_0^t e^{-a_S(t-\sigma)} \int_\Omega G_S(t-\sigma,\rho,y) \int_0^\sigma e^{-a_R(\sigma-s)} \times \int_\Omega G_R(\sigma-s,y,z)\Big(\int_0^s e^{-a_Q(s-w)} \int_\Omega G_Q(s-w,z,x) \times \Big[e^{-a_I w} \int_0^w q_I(\tau)\pi(\tau) \int_\Omega G_I(\tau,x,\theta) M_0(w-\tau,\theta) d\theta d\tau\Big] dx\, dw\Big) dz\, ds\, dy\, d\sigma,$$

$$L_4(M_0) = \int_0^t e^{-a_I t} \beta(\tau)\pi(\tau) \int_\Omega G_I(\tau,\rho,y) M_0(t-\tau,y)\, dy\, d\tau,$$

$$K_1(t,\rho) = K_3(t,\rho) + K_4(t,\rho) + K_5(t,\rho) + K_6(t,\rho),$$

$$K_2(t,\rho) = e^{-a_I t} \int_t^{\tau^+} \beta(\tau) \frac{\pi(\tau)}{\pi(\tau-t)} \int_\Omega G_I(t,\rho,y) I_0(\tau-t,y) dy d\tau,$$

$$K_3(t,\rho) = \delta \int_0^t e^{-a_S(t-\sigma)} \int_\Omega G_S(t-\sigma,\rho,y) R_1(\sigma,y)\, dy\, d\sigma,$$

$$K_4(t,\rho) = \delta \int_0^t e^{-a_S(t-\sigma)} \int_\Omega G_S(t-\sigma,\rho,y) \int_0^\sigma e^{-a_R(\sigma-s)} \int_\Omega G_R(\sigma-s,y,z) \times \Big[e^{-a_I s} \int_s^{\tau^+} \sigma_I(\tau) \frac{\pi(\tau)}{\pi(\tau-s)} \int_\Omega G_I(s,z,x) I_0(\tau-s,x)\, dx\, d\tau\Big] dz\, ds\, dy\, d\sigma,$$

$$K_5(t,\rho) = \sigma_Q \delta \int_0^t e^{-a_S(t-\sigma)} \int_\Omega G_S(t-\sigma,\rho,y) \int_0^\sigma e^{-a_R(\sigma-s)} \int_\Omega G_R(\sigma-s,y,z) Q_1(s,z)\, dz\, ds\, dy\, d\sigma,$$

$$K_6(t,\rho) = \sigma_Q \delta \int_0^t e^{-a_S(t-\sigma)} \int_\Omega G_S(t-\sigma,\rho,y) \int_0^\sigma e^{-a_R(\sigma-s)} \int_\Omega G_R(\sigma-s,y,z) \times \Big(\int_0^s e^{-a_Q(s-w)} \int_\Omega G_Q(s-w,z,x) \times \Big[e^{-a_I w} \int_w^{\tau^+} q_I(\tau) \frac{\pi(\tau)}{\pi(\tau-w)} \int_\Omega G_I(w,x,\theta) I_0(\tau-w,\theta) d\theta d\tau\Big] dx\, dw\Big) dz\, ds\, dy\, d\sigma.$$

Next, consider a space $Y_{T^*} = C([0,T^*],\mathbb{X})$ with the norm

$$\|\Gamma\|_{Y_{T^*}} = \sup_{t\in[0,T^*]} \Big(\sup_{x\in\overline{\Omega}} |\Gamma(t,\rho)| \Big),\ \Gamma \in Y_{T^*}.$$

Clearly, $(Y_{T^*}, \|\cdot\|_{Y_{T^*}})$ forms a Banach space. Define an operator $\mathcal{G} : Y_{T^*} \to Y_{T^*}$ by

$$\mathcal{G}(M_0) = \frac{1}{N}\Big(S_1 + L_1(M_0) + L_2(M_0) + L_3(M_0) + K_1\Big)\Big(K_2 + L_4(M_0)\Big). \tag{3.10}$$

Since $M_0(t,\rho)$ fully determines S, I, Q and R, and using (3.9), we can conclude that the operator $\mathcal{G}$ admits a fixed point, it follows that system (3.1) has at least one solution. Next, establishing the uniqueness of the solution to system (3.1) is equivalent to proving the uniqueness of the fixed point of the operator $\mathcal{G}$. We show that $\mathcal{G}$ is a contraction mapping. For any $\widetilde{M_0}, \overline{M_0} \in Y_{T^*}$, we have

$$\begin{aligned} N\Big(\mathcal{G}(\widetilde{M_0}) - \mathcal{G}(\overline{M_0})\Big) &= (S_1 + L_1(\widetilde{M_0}) + L_2(\widetilde{M_0}) + L_3(\widetilde{M_0}) + K_1)(K_2 + L_4(\widetilde{M_0})) \\ &\quad - (S_1 + L_1(\overline{M_0}) + L_2(\overline{M_0}) + L_3(\overline{M_0}) + K_1)(K_2 + L_4(\overline{M_0})) \\ &= (K_2 + L_4(\widetilde{M_0}))\Big[\sum_{i=1}^3 \Big(L_i(\widetilde{M_0}) - L_i(\overline{M_0})\Big)\Big] \end{aligned}$$

$$- (S_1 + L_1(\overline{M_0}) + L_2(\overline{M_0}) + L_3(\overline{M_0}) + K_1)\Big[L_4(\widetilde{M_0}) - L_4(\overline{M_0})\Big].$$

Using (3.3) and Assumption 2.2, we obtain

$$\begin{aligned}
|L_1(\widetilde{M_0}) - L_1(\overline{M_0})| &= \Big| \int_0^t e^{-a_S(t-\sigma)} \int_\Omega G_S(t-\sigma,\rho,y)[\overline{M_0}(\sigma,y) - \widetilde{M_0}(\sigma,y)]\,dy\,d\sigma \Big| \\
&\le \|\widetilde{M_0} - \overline{M_0}\|_{Y_{T^*}} \int_0^t e^{-a_S(t-\sigma)} d\sigma \\
&\le T^* \|\widetilde{M_0} - \overline{M_0}\|_{Y_{T^*}}.
\end{aligned}$$

Similarly, after some simple calculations, we obtain

$$\begin{aligned}
|L_2(\widetilde{M_0}) - L_2(\overline{M_0})| &\le \delta\sigma_I^M \frac{(T^*)^3}{6} \|\widetilde{M_0} - \overline{M_0}\|_{Y_{T^*}}, \\
|L_3(\widetilde{M_0}) - L_3(\overline{M_0})| &\le \delta\sigma_Q q_I^M \frac{(T^*)^4}{24} \|\widetilde{M_0} - \overline{M_0}\|_{Y_{T^*}}, \\
|L_4(\widetilde{M_0}) - L_4(\overline{M_0})| &\le \beta^M T^* \|\widetilde{M_0} - \overline{M_0}\|_{Y_{T^*}}.
\end{aligned}$$

Using these equations, we obtain

$$|\mathcal{G}(\widetilde{M_0}) - \mathcal{G}(\overline{M_0})| \le C(T^*) \|\widetilde{M_0} - \overline{M_0}\|_{Y_{T^*}},$$

where

$$\begin{aligned}
C(T^*) = \frac{1}{N} \| &\Big(K_2(T^*,\cdot) + L_4(\widetilde{M_0}(T^*,\cdot))\Big)\Big(T^* + \delta\sigma_I^M \frac{(T^*)^3}{6} + \delta\sigma_Q q_I^M \frac{(T^*)^4}{24}\Big) \\
&+ \beta^M T^* \Big(S_1(T^*,\cdot) + L_1(\overline{M_0}(T^*,\cdot)) + L_2(\overline{M_0}(T^*,\cdot)) + L_3(\overline{M_0}(T^*,\cdot)) + K_1(T^*,\cdot)\Big) \|_{\mathbb{X}}.
\end{aligned}$$

Since N is large, we can choose a sufficient T^* such that $C(T^*) < 1$. This ensures that the operator $\mathcal{G}$ is a contraction and therefore admits a unique fixed point. Hence, the system (3.1) admits a unique solution. □

4. Stability analysis

This section aims to determine whether small introductions of infection can invade and persist in the population, or whether they are eliminated over time. To this end, we identify a threshold quantity that captures the effects of infection-age-dependent transmission and spatial movement. This threshold separates regimes in which the disease-free equilibrium is stable from those in which sustained transmission occurs, thereby providing a rigorous criterion for disease elimination or persistence.

Note that the spatially homogeneous system corresponding to the system (3.1) is given by

$$\begin{aligned}
\frac{dS(t)}{dt} &= A - a_S S(t) - \frac{S(t)}{N} \int_0^{\tau^+} \beta(\tau) I(t,\tau)\,d\tau + \delta R(t), \\
\frac{\partial I(t,\tau)}{\partial \tau} + \frac{\partial I(t,\tau)}{\partial t} &= -(a_I + q_I(\tau) + \sigma_I(\tau) + d(\tau)) I(t,\tau), \\
\frac{dQ(t)}{dt} &= -a_Q Q(t) + \int_0^{\tau^+} q_I(\tau) I(t,\tau)\,d\tau, \\
\frac{dR(t)}{dt} &= -a_R R(t) + \sigma_Q Q(t) + \int_0^{\tau^+} \sigma_I(\tau) I(t,\tau)\,d\tau, \\
I(t,0) &= \frac{S(t)}{N} \int_0^{\tau^+} \beta(\tau) I(t,\tau)\,d\tau, \quad t \ge 0, \\
S(0) = S_0, &\quad I(0,\tau) = I_0(\tau), \quad Q(0) = Q_0,\ R(0) = R_0.
\end{aligned}$$

The disease-free equilibrium corresponding to (3.1) is $E^{DF} = \big(\frac{A}{a_S}, 0, 0, 0\big)$. Let $S^0 = \frac{A}{a_S}$ and linearizing the system (3.1) corresponding to E^{DF} gives

$$\begin{aligned}
\frac{\partial S(t,\rho)}{\partial t} &= d_S \Delta S(t,\rho) - \frac{S^0}{N}\int_0^{\tau^+} \beta(\tau) I(t,\tau,\rho)\, d\tau - a_S S(t,\rho) + \delta R(t,\rho),\\
\frac{\partial I(t,\tau,\rho)}{\partial \tau} + \frac{\partial I(t,\tau,\rho)}{\partial t} &= d_I \Delta I(t,\tau,\rho) - (a_I + m(\tau)) I(t,\tau,\rho),\\
\frac{\partial Q(t,\rho)}{\partial t} &= d_Q \Delta Q(t,\rho) - a_Q Q(t,\rho) + \int_0^{\tau^+} q_I(\tau) I(t,\tau,\rho)\, d\tau,\\
\frac{\partial R(t,\rho)}{\partial t} &= d_R \Delta R(t,\rho) - a_R R(t,\rho) + \int_0^{\tau^+} \sigma_I(\tau) I(t,\tau,\rho)\, d\tau + \sigma_Q Q(t,\rho),\\
I(t,0,\rho) &= \frac{S^0}{N}\int_0^{\tau^+} \beta(\tau) I(t,\tau,\rho)\, d\tau, \quad t \geq 0,\ \rho \in \Omega,\\
\frac{\partial S(t,\rho)}{\partial n} &= \frac{\partial I(t,\tau,\rho)}{\partial n} = \frac{\partial Q(t,\rho)}{\partial n} = \frac{\partial R(t,\rho)}{\partial n} = 0, \quad \rho \in \mathbb{R}^N \setminus \Omega,\\
S(0,\rho) &= S_0(\rho), \quad I(0,\tau,\rho) = I_0(\tau,\rho), \quad Q(0,\rho) = Q_0(\rho), \quad R(0,\rho) = R_0(\rho).
\end{aligned} \tag{4.1}$$

It follows that $M_0(t,\rho) = \frac{S^0}{N}\int_0^{\tau^+} \beta(\tau) I(t,\tau,\rho)\, d\tau$. Using (3.5) we obtain

$$\begin{aligned}
M_0(t,\rho) = \frac{S^0}{N}\Big[&\int_0^t \beta(\tau)\pi(\tau) e^{-a_I t} \int_\Omega G_I(\tau,\rho,y) M_0(t-\tau,y)\, dy\, d\tau\\
&+ \int_t^{\tau^+} \beta(\tau)\frac{\pi(\tau)}{\pi(t-\tau)} e^{-a_I t} \int_\Omega G_I(t,\rho,y) I_0(\tau - t, y)\, dy\, d\tau\Big].
\end{aligned} \tag{4.2}$$

To begin, our goal is to derive the next-generation operator $\mathcal{N}$, a crucial tool for characterizing the dynamics of new infections within the system. This operator provides insight into how infections propagate and evolve over time, serving as a foundation for computing key epidemiological metrics such as the basic reproduction number $\mathcal{R}_0$.

Remark 4.1. Observing the first component of the expression on the right-hand side of (4.2), we notice an important pattern: the number of new infections at any given time t is directly influenced by past infections. This relationship is formalized by the renewal equation, which describes how infections evolve based on previous cases. Hence, we obtain the next-generation operator $\mathcal{N} : \mathbb{X} \to \mathbb{X}$ by

$$\mathcal{N}[\Phi](\rho) = \frac{S^0}{N}\Big[\int_0^{\tau^+} \beta(\tau)\pi(\tau) e^{-a_I \tau} \int_\Omega G_I(\tau,\rho,y)\Phi(y)\, dy\, d\tau\Big]. \tag{4.3}$$

Following the foundational results in [7], we obtain $\mathcal{R}_0 = r(\mathcal{N})$, where $r(\mathcal{N})$ denotes the spectral radius of the operator $\mathcal{N}$. We want to apply the Krien-Rutman theorem to find $r(\mathcal{N})$. The next result states the basic requirement for the operator $\mathcal{N}$ to apply this theorem.

Lemma 4.2. *The operator $\mathcal{N}$ is positive and compact.*

Proof. It is straightforward to see that the operator $\mathcal{N}$ is positive. Specifically, if we take any Φ from the positive cone $\mathbb{X}_+$, Assumptions 2.2 ensures that $\mathcal{N}(\Phi) \in \mathbb{X}_+$. This confirms the positivity of $\mathcal{N}$. To establish that $\mathcal{N}$ is compact, we will apply the Arzelá-Ascoli theorem. Note that for each $\rho \in \overline{\Omega}$,

$$\|\mathcal{N}(\Phi)\|_{\mathbb{X}} \leq K\|\Phi\|_{\mathbb{X}} \quad \forall \Phi \in \mathbb{X},$$

where $K = \frac{S^0}{N}\beta^M \tau^+$. This shows that $\mathcal{N}$ is uniformly bounded.

Next, since Laplacian operator Δ is compact, the kernel $G_I(\tau,\rho,y)$ is uniformly continuous in ρ for $\rho \neq y$. Choose any $\rho, \tilde{\rho}(\neq y) \in \overline{\Omega}$ such that $|\rho - \tilde{\rho}| < \delta$ where $\delta = \min\{|\rho - y|, |\tilde{\rho} - y|\}$. Therefore, from uniform continuity of function G_I, for any $\epsilon' > 0$, we can find a corresponding $0 < \delta' < \delta$ such that whenever $|\rho - \tilde{\rho}| < \delta'$ we have

$$|G_I(\tau,\rho,y) - G_I(\tau,\tilde{\rho},y)| \leq \epsilon'.$$

Let $\{\Phi_n\} \subset \mathbb{X}$ be a sequence such that $|\Phi_n| \leq C$, for some $C > 0$ and for each $n \in \mathbb{N}$. Then for any $\rho, \tilde{\rho} \in \overline{\Omega}$ such that $|\rho - \tilde{\rho}| < \delta'$ we have

$$\Big|\mathcal{N}[\Phi_n](\rho) - \mathcal{N}[\Phi_n](\tilde{\rho})\Big| \leq \frac{CS^0}{N}\Big[\int_0^{\tau^+} \beta(\tau)\pi(\tau)e^{-a_I\tau}\int_\Omega \Big|G_I(\tau,\rho,y) - G_I(\tau,\tilde{\rho},y)\Big|\,dy\,d\tau\Big] \leq \epsilon,$$

where $\epsilon = \Big(\frac{CS^0\beta^M\tau^+|\Omega|}{N}\Big)\epsilon'$. This establishes the equicontinuity of the operator $\mathcal{N}$. Therefore, by applying the Arzelà-Ascoli theorem, we conclude that the operator $\mathcal{N}$ is compact. □

According to the Krein-Rutman Theorem [2], the operator $\mathcal{N}$ possesses a unique principal eigenvalue that is positive and corresponds to a strictly positive eigenvector. As a result, $\mathcal{R}_0$ is defined by

$$\mathcal{R}_0 = \frac{S^0}{N}\int_0^{\tau^+} \beta(\tau)\pi(\tau)e^{-a_I\tau}d\tau. \tag{4.4}$$

Remark 4.3. From (4.4), we observe that the basic reproduction number $\mathcal{R}_0$ is directly proportional to the recruitment rate A of susceptible individuals and inversely proportional to the vaccination rate v_S. This implies that increasing the influx of susceptible individuals into the population enhances the potential for disease transmission, while strengthening vaccination efforts suppresses the spread by reducing the pool of susceptibles. Consequently, controlling these two parameters plays a crucial role in pushing $\mathcal{R}_0$ below the threshold value of 1, thereby ensuring disease elimination.

Now, letting the endemic equilibrium of the system (3.1) be denoted by $E_* = (S_*, I_*(\tau), Q_*, R_*)$, then it satisfies

$$\begin{aligned}
A - I_*(0) - a_S S_* + \delta R_* &= 0,\\
\frac{dI_*(\tau)}{d\tau} &= -(m(\tau) + a_I)I_*(\tau),\\
\int_0^{\tau^+} q_I(\tau)I_*(\tau)\,d\tau - a_Q Q_* &= 0,\\
\int_0^{\tau^+} \sigma_I(\tau)I_*(\tau)\,d\tau + \sigma_Q Q_* - a_R R_* &= 0,\\
I_*(0) &= \frac{S_*}{N}\int_0^{\tau^+} \beta(\tau)I_*(\tau)\,d\tau.
\end{aligned} \tag{4.5}$$

From the last equation we obtain $S_* = S^0/\mathcal{R}_0$. Solving infected compartment gives $I_*(\tau) = I_*(0)\pi(\tau)e^{-a_I\tau}$. Using this we obtain $Q_* = \frac{I_*(0)}{a_Q}W_q$ and $R_* = \frac{I_*(0)}{a_R}\Big[\frac{\sigma_Q}{a_Q}W_q + W_\sigma\Big]$, where $W_q = \int_0^{\tau^+} q_I(\tau)\pi(\tau)e^{-a_I\tau}d\tau$ and $W_\sigma = \int_0^{\tau^+} \sigma_I(\tau)\pi(\tau)e^{-a_I\tau}d\tau$. Finally, we obtain $I_*(0) = \frac{A}{1-\omega}\big(1 - \frac{1}{\mathcal{R}_0}\big)$, where $w = \frac{\delta}{a_R}\big(\frac{\sigma_Q}{a_Q}W_q + W_\sigma\big)$. Using all this information, we have a result which provides an explicit characterization of the endemic equilibrium and outlines the conditions necessary for its existence.

Lemma 4.4. *When $\mathcal{R}_0 > 1$, the system described by* (3.1) *possesses a unique endemic steady state E_* characterized as follows:*

$$\begin{aligned}
S_* = \frac{S^0}{\mathcal{R}_0}, \quad I_*(\tau) &= \Big(\frac{A}{1-\omega}\Big)\pi(\tau)e^{-a_I\tau}\Big(1 - \frac{1}{\mathcal{R}_0}\Big),\\
Q_* = \frac{W_q}{a_Q}\Big(\frac{A}{1-\omega}\Big)\Big(1 - \frac{1}{\mathcal{R}_0}\Big), \quad R_* &= \frac{1}{\delta}\Big(\frac{A\omega}{1-\omega}\Big)\Big(1 - \frac{1}{\mathcal{R}_0}\Big).
\end{aligned} \tag{4.6}$$

We proceed to examine the stability of both equilibria by first applying the transformations

$$\tilde{S}(t,\rho) = S(t,\rho) - S_*, \quad \tilde{I}(t,\tau,\rho) = I(t,\tau,\rho) - I_*(\tau), \quad \tilde{Q}(t,\rho) = Q(t,\rho) - Q_*, \tilde{R}(t,\rho) = R(t,\rho) - R_*.$$

Then the linearized system corresponding to these transformations is

$$\begin{aligned}
\frac{\partial \tilde{S}(t,\rho)}{\partial t} &= d_S \Delta \tilde{S}(t,\rho) - \frac{S_*}{N}\int_0^{\tau^+} \beta(\tau)\tilde{I}(t,\tau,\rho)\,d\tau \\
&\quad - \frac{\tilde{S}(t,\rho)}{N}\int_0^{\tau^+} \beta(\tau)I_*(\tau)\,d\tau - a_S\tilde{S}(t,\rho) + \delta\tilde{R}(t,\rho), \\
\frac{\partial \tilde{I}(t,\tau,\rho)}{\partial t} + \frac{\partial \tilde{I}(t,\tau,\rho)}{\partial \tau} &= d_I \Delta \tilde{I}(t,\tau,\rho) - (m(\tau)+a_I)\tilde{I}(t,\tau,\rho), \\
\frac{\partial \tilde{Q}(t,\rho)}{\partial t} &= d_Q \Delta \tilde{Q}(t,\rho) + \int_0^{\tau^+} q_I(\tau)\tilde{I}(t,\tau,\rho)\,d\tau - a_Q\tilde{Q}(t,\rho), \\
\frac{\partial \tilde{R}(t,\rho)}{\partial t} &= d_R \Delta \tilde{R}(t,\rho) + \int_0^{\tau^+} \sigma_I(\tau)\tilde{I}(t,\tau,\rho)\,d\tau + \sigma_Q\tilde{Q}(t,\rho) - a_R\tilde{R}(t,\rho), \\
\tilde{I}(t,0,\rho) &= \frac{S_*}{N}\int_0^{\tau^+} \beta(\tau)\tilde{I}(t,\tau,\rho)\,d\tau + \frac{\tilde{S}(t,\rho)}{N}\int_0^{\tau^+} \beta(\tau)I_*(\tau)\,d\tau, \quad t\geq 0,\ \rho\in\Omega, \\
\frac{\partial \tilde{S}(t,\rho)}{\partial n} &= \frac{\partial \tilde{I}(t,\tau,\rho)}{\partial n} = \frac{\partial \tilde{Q}(t,\rho)}{\partial n} = \frac{\partial \tilde{R}(t,\rho)}{\partial n} = 0, \quad \rho\in\mathbb{R}^N\setminus\Omega, \\
\tilde{S}(0,\rho) &= \tilde{S}_0(\rho), \quad \tilde{I}(0,\tau,\rho) = \tilde{I}_0(\tau,\rho), \quad \tilde{Q}(0,\rho) = \tilde{Q}_0(\rho), \quad \tilde{R}(0,\rho) = \tilde{R}_0(\rho).
\end{aligned} \tag{4.7}$$

Next, we recall some basic spectral properties of the Laplace operator with homogeneous Neumann boundary conditions. According to [4], it is well known that the operator $-\Delta$ admits a sequence of nonnegative eigenvalues

$$0 \leq \lambda_0 \leq \lambda_1 \leq \lambda_2 \leq \cdots, \qquad \lambda_k \to +\infty,$$

with corresponding finite-dimensional eigenspaces

$$E(\lambda_k) = \{\phi \in C^\infty(\overline{\Omega}) : -\Delta\phi = \lambda_k\phi,\ \partial_n\phi = 0\}.$$

Each eigenspace $E(\lambda_k)$ is invariant under the semigroup generated by Δ. To study the stability of the steady state, we seek solutions of the linearized system of the form

$$\tilde{S}(t,\rho) = e^{\lambda t}\phi_1(\rho), \quad \tilde{I}(t,\tau,\rho) = e^{\lambda t}\phi_2(\tau,\rho), \quad \tilde{Q}(t,\rho) = e^{\lambda t}\phi_3(\rho), \quad \tilde{R}(t,\rho) = e^{\lambda t}\phi_4(\rho),$$

where $\lambda \in \mathbb{C}$ denotes the temporal growth rate.

Since the Laplacian admits invariant eigenspaces, the linearized system decouples with respect to the spectral modes of $-\Delta$. Therefore, without loss of generality, we restrict attention to solutions satisfying

$$\phi_1, \phi_3, \phi_4 \in E(\lambda_k)$$

for some fixed $k \geq 0$, and

$$\phi_2(\tau,\cdot) \in E(\lambda_k) \quad \text{for a.e. } \tau \in (0,\tau^+).$$

Consequently,

$$\Delta\phi_j = -\lambda_k\phi_j, \quad j = 1,3,4,$$

and pointwise in τ,

$$\Delta\phi_2(\tau,\rho) = -\lambda_k\phi_2(\tau,\rho), \quad \rho\in\Omega.$$

In particular, when $\dim E(\lambda_k) = 1$, there exists an eigenfunction φ_k such that

$$\phi_j(\rho) = c_j\varphi_k(\rho).$$

Substituting this ansatz into the linearized system yields a characteristic equation for the growth rate λ corresponding to each spatial mode λ_k. The local stability of the steady states is then determined by the sign of the real parts of the roots of these characteristic equations. Equation (4.7) with this solution form can be rewritten as

$$\begin{aligned}
&\lambda\phi_1(\rho) \\
&= -d_S\lambda_k\phi_1(\rho) - \frac{S_*}{N}\int_0^{\tau^+} \beta(\tau)\phi_2(\tau,\rho)\,d\tau - \frac{\phi_1(\rho)}{N}\int_0^{\tau^+} \beta(\tau)I_*(\tau)\,d\tau - a_S\phi_1(\rho) + \delta\phi_4(\rho),
\end{aligned} \tag{4.8a}$$

$$\frac{\partial \phi_2(\tau,\rho)}{\partial \tau} = -d_I\lambda_k\phi_2(\tau,\rho) - (m(\tau)+a_I+\lambda)\phi_2(\tau,\rho), \tag{4.8b}$$

$$\lambda\phi_3(\rho) = -d_Q\lambda_k\phi_3(\rho) + \int_0^{\tau^+} q_I(\tau)\phi_2(\tau,\rho)\,d\tau - a_Q\phi_3(\rho), \tag{4.8c}$$

$$\lambda\phi_4(\rho) = -d_R\lambda_k\phi_4(\rho) + \int_0^{\tau^+} \sigma_I(\tau)\phi_2(\tau,\rho)\,d\tau + \sigma_Q\phi_3(\rho) - a_R\phi_4(\rho), \tag{4.8d}$$

$$\phi_2(0,\rho) = \frac{S_*}{N}\int_0^{\tau^+} \beta(\tau)\phi_2(\tau,\rho)\,d\tau + \frac{\phi_1(\rho)}{N}\int_0^{\tau^+} \beta(\tau)I_*(\tau)\,d\tau, \quad t\geq 0,\ \rho\in\Omega. \tag{4.8e}$$

Solving equation (4.8b), we obtain

$$\phi_2(\tau,\rho) = \phi_2(0,\rho)\pi(\tau)e^{-(d_I\lambda_k+a_I+\lambda)\tau}.$$

Next, we establish that

$$\lambda \neq -(a_S+d_S\lambda_k-\delta), \quad \lambda\neq -(a_Q+d_Q\lambda_k), \quad \text{and} \quad \lambda\neq -(a_R+d_R\lambda_k).$$

Suppose, for the sake of contradiction, that

$$\lambda = -(a_S+d_S\lambda_k-\delta).$$

Then, from equation (4.8a), it follows that $\phi_2(0,\rho)=0$, which is a contradiction. Similarly, if we assume $\lambda=-(a_Q+d_Q\lambda_k)$, then substituting the expression for $\phi_2(\tau,\rho)$ into equation (4.8c) leads to $\phi_2(0,\rho)=0$, which is again a contradiction. By the same reasoning, we conclude that $\lambda\neq-(a_R+d_R\lambda_k)$. Now solving (4.8c) gives

$$\phi_3(\rho) = \frac{\phi_2(0,\rho)}{\lambda+d_Q\lambda_k+a_Q}\widehat{W_q},$$

where $\widehat{W_q}=\int_0^{\tau^+} q_I(\tau)\pi(\tau)e^{-(d_I\lambda_k+a_I+\lambda)\tau}d\tau$. Putting this in (4.8d) we obtain

$$\phi_4(\rho) = \frac{\phi_2(0,\rho)}{\lambda+d_R\lambda_k+a_R}\Big[\widehat{W_\sigma} + \frac{\sigma_Q}{\lambda+d_Q\lambda_k+a_Q}\widehat{W_q}\Big],$$

where $\widehat{W_\sigma}=\int_0^{\tau^+}\sigma_I(\tau)\pi(\tau)e^{-(d_I\lambda_k+a_I+\lambda)\tau}d\tau$. Finally, using the value of $\phi_4(\rho)$ in (4.8a) we obtain

$$\phi_1(\rho) = -\frac{\phi_2(0,\rho)}{\lambda+d_S\lambda_k+a_S}\Big(1-\frac{\delta}{\lambda+d_R\lambda_k+a_R}\Big[\widehat{W_\sigma}+\frac{\sigma_Q}{\lambda+d_Q\lambda_k+a_Q}\widehat{W_q}\Big]\Big).$$

Substituting $\phi_1(\rho)$ and $\phi_2(\tau,\rho)$ into (4.8e) yields an equation

$$\frac{S_*}{N}\widehat{W_\beta} = \Big[1+\frac{1}{N\kappa_S}\Big(1-\frac{\delta}{\kappa_R}\Big[\widehat{W_\sigma}+\frac{\sigma_Q}{\kappa_Q}\widehat{W_q}\Big]\Big)\int_0^{\tau^+}\beta(\tau)I_*(\tau)\,d\tau\Big], \tag{4.9}$$

where $\kappa_i=\lambda+d_i\lambda_k+a_i$ for $i=S,R,Q$, and $\widehat{W_\beta}=\int_0^{\tau^+}\beta(\tau)\pi(\tau)e^{-(d_I\lambda_k+a_I+\lambda)\tau}d\tau$. The eigenvalue problem (4.8a)-4.8e always possesses a principal eigenvalue, denoted by λ_*, which is the root of the equation (4.9) (refer to [28, 10] for further details). This eigenvalue plays a crucial role in analyzing the stability of both the disease-free (E^{DF}) and endemic (E_*) equilibria. We state the following theorem regarding the local asymptotic stability of these equilibria.

Theorem 4.5. *Under Assumptions 2.2 and 2.3, the disease-free equilibrium E^{DF} is locally asymptotically stable in the sense of linearized (spectral) stability if $\mathcal{R}_0<1$, while the endemic equilibrium E_* is locally asymptotically stable in the sense of linearized (spectral) stability if $\mathcal{R}_0>1$.*

Proof. Note that for E^{DF}, we have $I_*(\tau)=0$ and $S_*=S^0$. Thus (4.9) becomes

$$\frac{S^0}{N}\int_0^{\tau^+}\beta(\tau)\pi(\tau)e^{-(d_I\lambda_k+a_I+\lambda)\tau}d\tau = 1. \tag{4.9}$$

Suppose $\lambda=w_1+iw_2$ with $w_1\geq 0$ is a root of the equation (4.9). Then we obtain

$$\Big|\frac{S^0}{N}\int_0^{\tau^+}\beta(\tau)\pi(\tau)e^{-(d_I\lambda_k+a_I+\lambda)\tau}d\tau\Big| \leq \frac{S^0}{N}\int_0^{\tau^+}\beta(\tau)\pi(\tau)e^{-a_I\tau}\big|e^{-iw_2\tau}\big|d\tau = \mathcal{R}_0.$$

Whenever $\mathcal{R}_0 < 1$, we obtain

$$\Big|\frac{S^0}{N}\int_0^{\tau^+}\beta(\tau)\pi(\tau)e^{-(d_I\lambda_k+a_I+\lambda)\tau}d\tau\Big| < 1,$$

which is a contradiction to (4.9). Thus, all roots of equation (4.9) possess negative real parts whenever $\mathcal{R}_0 < 1$. Consequently, E^{DF} is locally asymptotically stable under this condition.

For the other case, when $\mathcal{R}_0 > 1$, from Lemma 4.4, there exists a unique positive endemic equilibrium point. For this equilibrium point, assume $\lambda = x_1 + ix_2$, with $x_1 > 0$, is the root of the equation (4.9). The right-hand side of the equation (4.9) becomes

$$\Big|\frac{S_*}{N}\widehat{W_\beta}\Big| = \Big|\frac{1}{\mathcal{R}_0}\Big(\frac{S^0}{N}\int_0^{\tau^+}\beta(\tau)\pi(\tau)e^{-(d_I\lambda_k+a_I+\lambda)\tau}d\tau\Big)\Big| \le 1. \tag{4.11}$$

Now, letting $P = \frac{\delta}{\lambda+d_R\lambda_k+a_R}\Big[\widehat{W_\sigma} + \frac{\sigma_Q}{\lambda+d_Q\lambda_k+a_Q}\widehat{W_q}\Big]$, then using values of a_Q and a_R, we obtain

$$\begin{aligned}
|P| &\le |\widehat{W_\sigma} + \widehat{W_q}| \\
&= \Big|\int_0^{\tau^+}\sigma_I(\tau)\pi(\tau)e^{-(d_I\lambda_k+a_I+\lambda)\tau}d\tau + \int_0^{\tau^+} q_I(\tau)\pi(\tau)e^{-(d_I\lambda_k+a_I+\lambda)\tau}d\tau\Big| \\
&\le (\sigma_I^M + q_I^M)\int_0^{\tau^+}|e^{iy\tau}|d\tau.
\end{aligned}$$

Thus, from Assumption 2.3, we obtain $|P| < 1$. Using this on the left-hand side of the equation (4.9), we obtain

$$\Big|1 + \frac{1}{N(\lambda+d_S\lambda_k+a_S)}\Big(1 - \frac{\delta}{\lambda+d_R\lambda_k+a_R}\Big[\widehat{W_\sigma} + \frac{\sigma_Q}{\lambda+d_Q\lambda_k+a_Q}\widehat{W_q}\Big]\Big)\int_0^{\tau^+}\beta(\tau)I_*(\tau)\,d\tau\Big| > 1,$$

which is a contradiction to (4.11). Hence λ must have a negative real part and therefore the endemic equilibrium is locally asymptotically stable whenever $\mathcal{R}_0 > 1$. □

Remark 4.6. The stability results in Theorem 4.5 are understood in the sense of linearized (spectral) stability. That is, the conclusions are based on the spectral properties of the linearized system (equivalently, of the generator of the associated linear semigroup) around the equilibrium. A rigorous extension of these results to nonlinear asymptotic stability would require the application of a principle of linearized stability for semilinear evolution equations, which is beyond the scope of this work.

5. Optimal control

In this section, we study the optimal control problem. We have adopted three major control measures: Social distancing among the susceptible population, quarantining the infected population, and vaccinating susceptible and infected individuals. We define the time domain as $[0, T]$, which allows policymakers or researchers to assess outcomes over a relevant time frame. To better reflect the impact of control measures and make the analysis more manageable, we make the following adjustments to the model (2.1):

(1) In model (2.1), the integral term $\int_0^{\tau^+}\beta(\tau)I(t,\tau,\rho)\,d\tau$ represents the *force of infection*, capturing the overall transmission potential contributed by infected individuals at various stages of their infection. To incorporate control strategies, we replace $\beta(\tau)$ with $a(t)b(\tau)$, where $a(t)$ reflects the rate of effective contacts per person at time t, and $b(\tau)$ accounts for how infectiousness changes with the time since infection τ. This reformulation enables the model to reflect changes in transmission patterns caused by seasonality, public health measures, or evolving behavior over time.
(2) We assume the susceptible influx $A = 0$. This can be justified by considering either a closed population with no births or immigration, or a short-term analysis where demographic changes are negligible.

(3) Instead of constant vaccination rates, we take time-dependent rates ($v_S(t)$ and $v_R(t)$). Incorporating time-dependent vaccination rates allows the model to capture dynamic intervention strategies realistically, reflecting variations in public health responses over time. This enhances predictive accuracy and enables optimal allocation of limited resources through adaptive control.

(4) To simplify analysis and enhance interpretability, we non-dimensionalize the model by rescaling each compartment as a proportion of the total population N. We use the transformations:

$$s(t,\rho)=\frac{S(t,\rho)}{N},\quad i(t,\tau,\rho)=\frac{I(t,\tau,\rho)}{N},\quad q(t,\rho)=\frac{Q(t,\rho)}{N},\quad r(t,\rho)=\frac{R(t,\rho)}{N},\quad v(t,\rho)=\frac{V(t,\rho)}{N}.$$

Next, we impose regularity conditions on the functions $a(t)$ and $b(\tau)$ to ensure biological realism and mathematical tractability.

Assumption 5.1. $a(t)$ is non-negative and $a\in C([0,T])$. Also $b\in L^\infty_+(0,\tau^+)$. Let $a^M=\sup\{a(t):t\in[0,T]\}$ and $b^M=\sup\{b(\tau):\tau\in(0,\tau^+)\}$.

Remark 5.2. These assumptions are essential for both biological and mathematical reasons. The continuity of $a(t)$ allows the model to capture gradual changes in contact behavior and ensures compatibility with semigroup methods. The boundedness of $b(\tau)$ keeps the force of infection well-defined and prevents unbounded growth in the system, supporting the existence and uniqueness of solutions.

There is an additional assumption regarding the regularity of $v_S(t)$ and $v_R(t)$.

Assumption 5.3. The vaccination rate of susceptible and recovered individuals $v_S(t)$ and $v_R(t)$, respectively, is assumed to be non-negative and continuous functions on the interval C([0, T]). Let $v_S^M=\sup\{v_S(t):t\in[0,T]\}$ and $v_R^M=\sup\{v_R(t):t\in[0,T]\}$.

With these adjustments, our optimal control problem becomes

$$\begin{aligned}
\frac{\partial s(t,\rho)}{\partial t}&=d_S\Delta s(t,\rho)-v_S(t)s(t,\rho)-s(t,\rho)\int_0^{\tau^+}b(\tau)i(t,\tau,\rho)\,d\tau+\delta r(t,\rho),\\
\frac{\partial i(t,\tau,\rho)}{\partial\tau}+\frac{\partial i(t,\tau,\rho)}{\partial t}&=d_I\Delta i(t,\tau,\rho)-m(\tau)i(t,\tau,\rho),\\
\frac{\partial q(t,\rho)}{\partial t}&=d_Q\Delta q(t,\rho)-\sigma_Q q(t,\rho)+\int_0^{\tau^+}q_I(\tau)i(t,\tau,\rho)\,d\tau,\\
\frac{\partial r(t,\rho)}{\partial t}&=d_R\Delta r(t,\rho)-(v_R(t)+\delta)r(t,\rho)+\int_0^{\tau^+}\sigma_I(\tau)i(t,\tau,\rho)\,d\tau+\sigma_Q q(t,\rho),\\
\frac{\partial v(t,\rho)}{\partial t}&=d_V\Delta v(t,\rho)+v_S(t)s(t,\rho)+v_R(t)r(t,\rho),\\
i(t,0,\rho)&=a(t)s(t,\rho)\int_0^{\tau^+}b(\tau)i(t,\tau,\rho)\,d\tau,\ t\ge0,\ \rho\in\Omega,\\
\frac{\partial s(t,\rho)}{\partial n}&=\frac{\partial i(t,\tau,\rho)}{\partial n}=\frac{\partial q(t,\rho)}{\partial n}=\frac{\partial r(t,\rho)}{\partial n}=\frac{\partial v(t,\rho)}{\partial n}=0,\ \rho\in\mathbb{R}^N\setminus\Omega,\\
s(0,\rho)&=s_0(\rho),\ i(0,\tau,\rho)=i_0(\tau,\rho),\ q(0,\rho)=q_0(\rho),\ r(0,\rho)=r_0(\rho),\ v(0,\rho)=v_0(\rho).
\end{aligned}\tag{5.1}$$

Next, we construct the objective functional. Our primary goal is to reduce the spread of infection by promoting social distancing, which is modelled by minimizing the contact rate $a(t)$ between susceptible and infected individuals. At the same time, we consider the costs associated with applying control measures. Taking both objectives into account, we define the following functional to be minimized,

$$\begin{aligned}
\mathcal{F}(a,v_S,v_R,q_I)=&\int_0^T\int_0^{\tau^+}\int_\Omega A_1 i(t,\tau,\rho)\,d\rho\,d\tau\,dt\\
&+\int_0^T\frac{1}{2}\Big(A_2v_S^2(t)+A_3v_R^2(t)+A_4a^2(t)\Big)dt+\int_0^{\tau^+}\frac{1}{2}A_5q_I^2(\tau)\,d\tau,
\end{aligned}\tag{5.2}$$

where the constants A_1, A_2, A_3, A_4, A_5 represents weighing factors. We define the control set as

$$\begin{aligned}\mathcal{U} = \big\{(a, v_S, v_R, q_I) :\ & a, v_S, v_R \in L^\infty(0,T), q_I \in L^\infty(0,\tau^+), 0 \le a(t) \le a^M, \\ & 0 \le v_S(t) \le v_S^M,\ 0 \le v_R(t) \le v_R^M,\ 0 \le q_I(\tau) \le q_I^M\big\}.\end{aligned} \tag{5.3}$$

5.1. **Regularity and boundedness of state trajectories.** To establish convergence and ensure the existence of an optimal control for our model, it is essential to derive estimates for the norms of the system's state variables (we refer to [8] for further details). These estimates are presented in Theorem 5.9. Before presenting that result, we demonstrate that system (5.1) admits a solution that can be readily established using semigroup theory.

Let $\mathcal{D}_1 = (0,\tau^+) \times \Omega$ and $\mathcal{D}_2 = [0,T] \times \Omega$. We define the functional spaces $H_1 = L^2(\Omega)$ and $H_2 = L^2(\mathcal{D}_1)$. Based on these, we introduce the product space

$$H := H_1 \times H_2 \times H_1 \times H_1 \times H_1 \times \{0\},$$

which will serve as the state space for our system. The associated positive cone is defined as

$$H_+ := H_{1+} \times H_{2+} \times H_{1+} \times H_{1+} \times H_{1+} \times \{0\},$$

where H_{1+} and H_{2+} are positive cones in H_1 and H_2, respectively.

Let $\widehat{\eta_1} = (\eta_{1_1}, \eta_{1_2}, \eta_{1_3}, \eta_{1_4}, \eta_{1_5}, 0) \in H$ and $\widehat{\eta_2} = (\eta_{2_1}, \eta_{2_2}, \eta_{2_3}, \eta_{2_4}, \eta_{2_5}, 0) \in H$, the inner product on H is defined as

$$\langle \widehat{\eta_1}, \widehat{\eta_2} \rangle_H = \langle \eta_{1_1}, \eta_{2_1} \rangle_{H_1} + \langle \eta_{1_2}, \eta_{2_2} \rangle_{H_2} + \langle \eta_{1_3}, \eta_{2_3} \rangle_{H_1} + \langle \eta_{1_4}, \eta_{2_4} \rangle_{H_1} + \langle \eta_{1_5}, \eta_{2_5} \rangle_{H_1},$$

where $\langle \cdot, \cdot \rangle_{H_1}$ and $\langle \cdot, \cdot \rangle_{H_2}$ denote the usual inner product on $H_1 = L^2(\Omega)$ and $H_2 = L^2(\mathcal{D}_1)$, respectively. It is easy to check that with this inner product, H forms a Hilbert space. Define a linear operator $\mathcal{A} : D(\mathcal{A}) \subseteq H \to H$ by

$$\mathcal{A}(\eta) = \Big\{ d_S \Delta\eta_1(\rho), d_I \Delta\eta_2(\tau,\rho) - \frac{\partial \eta_2(\tau,\rho)}{\partial \tau}, d_Q \Delta\eta_3(\rho), d_R \Delta\eta_4(\rho), d_V \Delta\eta_5(\rho), 0 \Big\}^T, \tag{5.4}$$

where $\eta = \{\eta_1, \eta_2, \eta_3, \eta_4, \eta_5, 0\} \in H$ and domain of the operator $\mathcal{A}$ is given by

$$D(\mathcal{A}) = \{\eta \in H : \Delta\eta \in H, \frac{\partial \eta_2}{\partial \tau} \in H_2, \frac{\partial \eta_i}{\partial n}\Big|_{\rho \in \mathbb{R}^N \setminus \Omega} = 0 \quad (i = 1, \dots, 5)\}.$$

Next, we define the non-linear operator $\mathcal{P} : [0,T] \times H \to H$ as follows:

$$\mathcal{P}(t,\eta) = \begin{pmatrix} -a(t)\eta_1(\rho)(\mathcal{P}_1\eta_2)(\rho) - v_S(t)\eta_1(\rho) + \delta\eta_4(\rho) \\ -m(\tau)\eta_2(\tau,\rho) \\ (\mathcal{P}_2\eta_2)(\rho) - \sigma_Q\eta_3(\rho) \\ (\mathcal{P}_3\eta_2)(\rho) + \sigma_Q\eta_3(\rho) - (v_R(t) + \delta)\eta_4(\rho) \\ v_S(t)\eta_1(\rho) + v_R(t)\eta_4(\rho) \\ a(t)\eta_1(\rho)(\mathcal{P}_1\eta_2)(\rho) - \eta_2(0,\rho) \end{pmatrix}, \tag{5.5}$$

where

$$\begin{aligned}(\mathcal{P}_1\eta_2)(\cdot) &= \int_0^{\tau^+} b(\tau)\eta_2(\tau,\cdot)\, d\tau, \\ (\mathcal{P}_2\eta_2)(\cdot) &= \int_0^{\tau^+} q_I(\tau)\eta_2(\tau,\cdot)\, d\tau, \\ (\mathcal{P}_3\eta_2)(\cdot) &= \int_0^{\tau^+} \sigma_I(\tau)\eta_2(\tau,\cdot)\, d\tau.\end{aligned}$$

Under this formulation, if we set $w = (s, i, q, r, v, 0) \in H$, the system (5.1) can be expressed as an abstract Cauchy problem

$$\begin{aligned}\frac{dw}{dt} &= \mathcal{A}w(t) + \mathcal{P}(t, w(t)), \\ w(0) &= w_0 \in H_+.\end{aligned} \tag{5.6}$$

Next, we have the following result for the nonlinear operator $\mathcal{P}$ for the well-posedness of a mild solution of the system (5.6).

Lemma 5.4. *Under Assumptions 2.2, 5.1 and 5.3, the operator $\mathcal{P}$ is*

(1) *locally Lipschitz continuous in w for all $t \in [0,T]$;*
(2) *measurable in t for all $w \in H$.*

Moreover, there exists a constant $C > 0$ such that $\mathcal{P}$ satisfies the growth condition

$$\|\mathcal{P}(t,w)\|_H \le C(1 + \|w\|_H), \quad \text{for all } t \in [0,T], w \in H. \tag{5.7}$$

Proof. The local Lipschitz continuity follows directly from the Assumptions 2.2, 5.1 and 5.3. Also, continuity of the functions $a(t), v_S(t)$ and $v_R(t)$ guarantees that the operator $\mathcal{P}$ is measurable in t for all $w \in H$. Using boundedness of $b(\tau)$ and Minkowski's inequality we obtain

$$\|(\mathcal{P}_1 i)\|_{H_1} \le b^M (\tau^+)^{1/2} \|i\|_{H_2}.$$

Similarly, $\|(\mathcal{P}_2 i)\|_{H_1} \le q_I^M (\tau^+)^{1/2} \|i\|_{H_2}$ and $\|(\mathcal{P}_3 i)\|_{H_1} \le \sigma_I^M (\tau^+)^{1/2} \|i\|_{H_2}$. Let the first component of the operator $\mathcal{P}$ as

$$\widetilde{P_1}(t,w) = -a(t)s(\rho)(\mathcal{P}_1 i)(\rho) - v_S(t)s(\rho) + \delta r(\rho).$$

Then using $0 \le s(t,\rho) \le 1$, we obtain

$$\begin{aligned}
\|\widetilde{P_1}\|_{[0,T]\times H_1} &\le a^M (\|s\|_{H_1}.\|\mathcal{P}_1 i\|_{H_1}) + v_S^M \|s\|_{H_1} + \delta \|r\|_{H_1} \\
&\le a^M.b^M (\tau^+)^{1/2} \|i\|_{H_2} + v_S^M \|s\|_{H_1} + \delta \|r\|_{H_1} \\
&\le C_1(\|s\|_{H_1} + \|i\|_{H_2} + \|r\|_{H_1}) \\
&\le C_1 \|w\|_H
\end{aligned}$$

where $C_1 = \frac{1}{3}\max\{v_S^M, (a.b)^M (\tau^+)^{1/2}, \delta\}$. Proceeding in the same way for the other components of $\mathcal{P}$, we obtain the inequality (5.7) for some constant $C > 0$. □

Remark 5.5. The growth condition on $\mathcal{P}$ prevents finite-time blow-up by ensuring the nonlinear term doesn't grow too rapidly compared to the linear dissipative effects. Without this bound, solutions could become unbounded in finite time. A linear growth condition guarantees global extendability of mild solutions.

Remark 5.6. From (5.7) note that we include a constant term alongside the norm to ensure the estimate holds uniformly, especially when w is small or zero. This captures any fixed contributions that may arise in $\mathcal{P}(t,w)$ regardless of the size of w.

Lemma 5.7. *The operator $\mathcal{A}$ defined in* (5.4) *generates a C_0 semigroup denoted by T_A.*

This result, and Lemma 5.4, establish the existence of a mild solution to the system (5.6).

Theorem 5.8. *Under the Assumptions 2.2, 2.3 and 5.3, for any initial condition $w_0 \in H_+$, the abstract Cauchy problem* (5.6) *admits a unique global mild solution*

$$w \in C([0,T]; H),$$

for any finite time $T > 0$. Moreover, the solution is given by

$$w(t) = T_A(t)w_0 + \int_0^t T_A(t-s)\mathcal{P}(s, w(s))ds.$$

Motivated by the approaches in [13, 6], the following result establishes the uniform boundedness and existence of strong solutions to the control system described by equation (5.1).

Theorem 5.9. *Under Assumptions 2.2, 2.3 and 5.3, if the initial data $w_0 \in D(\mathcal{A}) \cap H_+$, the abstract Cauchy problem* (5.6) *admits a unique strong solution $w = (s, i, q, r, v, 0)$ such that*

$$s, q, r, v \in X_1 \cap X_2 \cap X_3 \quad \text{and} \quad i \in L^2((0,\tau^+); X_1) \cap L^\infty((0,\tau^+); X_2) \cap L^\infty(\mathcal{D}_3),$$

where $X_1 = L^2(0,T; H^2(\Omega))$, $X_2 = L^\infty(0,T; H^1(\Omega))$, $X_3 = L^\infty(\mathcal{D}_2)$ and $\mathcal{D}_3 = [0,T] \times (0,\tau^+) \times \Omega$. Moreover, there exist a constant $\mathcal{K} > 0$ independent of the control variables a, v_S, v_R and q_I such

that

$$\begin{aligned}
\|\frac{\partial s}{\partial t}\|_{L^2(\mathcal{D}_2)} + \|s\|_{X_1} + \|s(t)\|_{H^1(\Omega)} + \|s\|_{X_3} &\le \mathcal{K},\\
\|\frac{\partial q}{\partial t}\|_{L^2(\mathcal{D}_2)} + \|q\|_{X_1} + \|q(t)\|_{H^1(\Omega)} + \|q\|_{X_3} &\le \mathcal{K},\\
\|\frac{\partial r}{\partial t}\|_{L^2(\mathcal{D}_2)} + \|r\|_{X_1} + \|r(t)\|_{H^1(\Omega)} + \|r\|_{X_3} &\le \mathcal{K},\\
\|\frac{\partial v}{\partial t}\|_{L^2(\mathcal{D}_2)} + \|v\|_{X_1} + \|v(t)\|_{H^1(\Omega)} + \|v\|_{X_3} &\le \mathcal{K},\\
\|\frac{\partial i}{\partial t}\|_{L^2(\mathcal{D}_3)} + \|\frac{\partial i}{\partial \tau}\|_{L^2(\mathcal{D}_3)} + \|i\|_{Y_1} + \|i(t)\|_{X_2} + \|i\|_{Y_3} &\le \mathcal{K},
\end{aligned} \tag{5.8}$$

where $Y_1 = L^2((0,\tau^+); X_1)$ *and* $Y_3 = L^\infty(\mathcal{D}_3)$.

We end this subsection by giving a remark justifying the regularity obtained in Theorem 5.9.

Remark 5.10. In the above theorem, the spatial H^2-regularity of the system's state is obtained using parabolic regularity theory. The L^2-based estimates follow from standard energy methods, while the L^∞ bounds are derived using the maximum principle or the inherent boundedness of the state variables.

5.2. **Derivation of necessary conditions for optimality.** In this subsection, we derive the first-order necessary conditions that must be satisfied for the existence of an optimal control.

Let $\mathcal{H} = (h_1, h_2, h_3, h_4)$ where $h_1, h_2, h_3 \in L^\infty([0,T])$ and $h_4 \in L^\infty(0,\tau^+)$. For $0 < \epsilon < 1$, we define

$$a^\epsilon(t) = a(t) + \epsilon h_1(t), \quad v_S^\epsilon(t) = v_S(t) + \epsilon h_2(t), \quad v_R^\epsilon(t) = v_R(t) + \epsilon h_3(t), \quad q_I^\epsilon(\tau) = q_I(\tau) + \epsilon h_4(\tau).$$

Let $U^\epsilon = (a^\epsilon, v_S^\epsilon, v_R^\epsilon, q_I^\epsilon)$ and $U = (a, v_S, v_R, q_I)$. To compute the derivative of the objective functional $\mathcal{F}$, it is necessary that the mapping $(a, v_S, v_R, q_I) \to (s,i,q,r,v)[a, v_S, v_R, q_I]$ be differentiable. According to Theorem 5.9, the map is Lipschitz continuous. Therefore, based on the results in [3], it follows that the map is differentiable, and we can define the Gâteaux derivatives $\overline{s}, \overline{i}, \overline{q}, \overline{r}$ and $\overline{v}$ such that

$$\lim_{\epsilon\to 0}\Big[\frac{(s,i,q,r,v)[U^\epsilon] - (s,i,q,r,v)[U]}{\epsilon}\Big] = (\overline{s}, \overline{i}, \overline{q}, \overline{r}, \overline{v}).$$

Hence, the directional derivative of $\mathcal{F}$ at U in the direction of $\mathcal{H}$ is

$$\begin{aligned}
&\mathcal{F}'(a, v_S, v_R, q_I)\\
&= \int_0^T \int_0^{\tau^+} \int_\Omega A_1 \overline{i}(t,\tau,\rho)\, d\rho\, d\tau\, dt + \int_0^T \Big(A_2 v_S(t) h_2(t) + A_3 v_R(t) h_3(t) + A_4 a(t) h_1(t)\Big) dt\\
&\quad + \int_0^{\tau^+} A_5 q_I(\tau) h_4(\tau)\, d\tau.
\end{aligned} \tag{5.9}$$

The variational linearized system that governs the derivatives $(\overline{s}, \overline{i}, \overline{q}, \overline{r}, \overline{v})$ is

$$\begin{aligned}
\frac{\partial \overline{s}(t,\rho)}{\partial t} &= d_S \Delta \overline{s}(t,\rho) - a(t) s(t,\rho) \int_0^{\tau^+} b(\tau)\overline{i}(t,\tau,\rho)\, d\tau - a(t)\overline{s}(t,\rho) \int_0^{\tau^+} b(\tau) i(t,\tau,\rho)\, d\tau\\
&\quad - h_1(t) s(t,\rho) \int_0^{\tau^+} b(\tau) i(t,\tau,\rho)\, d\tau - v_S(t)\overline{s}(t,\rho) - h_2(t) s(t,\rho) + \delta \overline{r}(t,\rho),\\
\frac{\partial \overline{i}(t,\tau,\rho)}{\partial \tau} + \frac{\partial \overline{i}(t,\tau,\rho)}{\partial t} &= d_I \Delta \overline{i}(t,\tau,\rho) - m(\tau)\overline{i}(t,\tau,\rho) - h_4(\tau) i(t,\tau,\rho),\\
\frac{\partial \overline{q}(t,\rho)}{\partial t} &= d_Q \Delta \overline{q}(t,\rho) + \int_0^{\tau^+} q_I(\tau)\overline{i}(t,\tau,\rho)\, d\tau + \int_0^{\tau^+} h_4(\tau) i(t,\tau,\rho)\, d\tau - \sigma_Q \overline{q}(t,\rho),\\
\frac{\partial \overline{r}(t,\rho)}{\partial t} &= d_R \Delta \overline{r}(t,\rho) + \int_0^{\tau^+} \sigma_I(\tau)\overline{i}(t,\tau,\rho)\, d\tau + \sigma_Q \overline{q}(t,\rho) - (v_R(t) + \delta)\overline{r}(t,\rho) - h_3(t) r(t,\rho),
\end{aligned}$$

$$
\begin{aligned}
\frac{\partial \overline{v}(t,\rho)}{\partial t} &= d_V \Delta \overline{v}(t,\rho) + v_S(t)\overline{s}(t,\rho) + h_2(t)s(t,\rho) + v_R(t)\overline{r}(t,\rho) + h_3(t)r(t,\rho),\\
\overline{i}(t,0,\rho) &= a(t)s(t,\rho)\int_0^{\tau^+} b(\tau)\overline{i}(t,\tau,\rho)\,d\tau + a(t)\overline{s}(t,\rho)\int_0^{\tau^+} b(\tau)i(t,\tau,\rho)\,d\tau\\
&\quad + h_1(t)s(t,\rho)\int_0^{\tau^+} b(\tau)i(t,\tau,\rho)\,d\tau, \quad t\geq 0,\ \rho\in\Omega,\\
\frac{\partial \overline{s}(t,\rho)}{\partial n} &= \frac{\partial \overline{i}(t,\tau,\rho)}{\partial n} = \frac{\partial \overline{q}(t,\rho)}{\partial n} = \frac{\partial \overline{r}(t,\rho)}{\partial n} = \frac{\partial \overline{v}(t,\rho)}{\partial n} = 0, \quad \rho\in\mathbb{R}^N\setminus\Omega,\\
\overline{s}(0,\rho) &= \overline{s}_0(\rho), \quad \overline{i}(0,\tau,\rho) = \overline{i}_0(\tau,\rho), \quad \overline{q}(0,\rho) = \overline{q}_0(\rho), \quad \overline{r}(0,\rho) = \overline{r}_0(\rho), \quad \overline{v}(0,\rho) = \overline{v}_0(\rho).
\end{aligned}
$$

Our next goal is to derive the adjoint system associated with the control system given in (5.1). Let $Y_1 = L^2(\mathcal{D}_2)$ and $Y_2 = L^2(\mathcal{D}_3)$. Then

$$
\begin{aligned}
&\Big\langle \frac{\partial \overline{s}(t,\rho)}{\partial t} - d_S\Delta\overline{s}(t,\rho) + a(t)s(t,\rho)\int_0^{\tau^+} b(\tau)\overline{i}(t,\tau,\rho)\,d\tau + a(t)\overline{s}(t,\rho)\int_0^{\tau^+} b(\tau)i(t,\tau,\rho)\,d\tau\\
&+ h_1(t)s(t,\rho)\int_0^{\tau^+} b(\tau)i(t,\tau,\rho)\,d\tau + v_S(t)\overline{s}(t,\rho) + h_2(t)s(t,\rho) - \delta\overline{r}(t,\rho), s^*(t,\rho)\Big\rangle_{Y_1} = 0,\\
&\Big\langle \overline{s}(t,\rho), -\Big(\frac{\partial s^*(t,\rho)}{\partial t} + d_S\Delta s^*(t,\rho) - a(t)s^*(t,\rho)\int_0^{\tau^+} b(\tau)i(t,\tau,\rho)\,d\tau - v_S(t)s^*(t,\rho)\Big)\Big\rangle_{Y_1}\\
&+ \int_0^T\int_\Omega \Big(a(t)s(t,\rho)\int_0^{\tau^+} b(\tau)\overline{i}(t,\tau,\rho)\,d\tau + h_1(t)s(t,\rho)\int_0^{\tau^+} b(\tau)i(t,\tau,\rho)\,d\tau\Big)s^*(t,\rho)d\rho dt\\
&+ \int_0^T\int_\Omega h_2(t)s(t,\rho)s^*(t,\rho)d\rho dt - \int_0^T\int_\Omega \delta\overline{r}(t,\rho)s^*(t,\rho)d\rho dt = 0.
\end{aligned}
\tag{5.10}
$$

By applying the same procedure to the remaining state variables, we obtain

$$
\Big\langle \frac{\partial \overline{i}(t,\tau,\rho)}{\partial \tau} + \frac{\partial \overline{i}(t,\tau,\rho)}{\partial t} - d_I\Delta\overline{i}(t,\tau,\rho) + m(\tau)\overline{i}(t,\tau,\rho) + h_4(\tau)i(t,\tau,\rho), i^*(t,\tau,\rho)\Big\rangle_{Y_2} = 0, \tag{5.11}
$$

$$
\begin{aligned}
&\Big\langle \overline{i}(t,\tau,\rho), -\Big(\frac{\partial i^*(t,\tau,\rho)}{\partial \tau} + \frac{\partial i^*(t,\tau,\rho)}{\partial t} + d_I\Delta i^*(t,\tau,\rho) - m(\tau)i^*(t,\tau,\rho)\Big)\Big\rangle_{Y_2}\\
&+ \int_0^T\int_0^{\tau^+}\int_\Omega h_4(\tau)i(t,\tau,\rho)i^*(t,\tau,\rho)\,d\rho\,d\tau\,dt = 0.
\end{aligned}
\tag{5.12}
$$

$$
\begin{aligned}
&\Big\langle \Big(\frac{\partial}{\partial t} - d_Q\Delta\Big)\overline{q}(t,\rho) - \int_0^{\tau^+} q_I(\tau)\overline{i}(t,\tau,\rho)\,d\tau - \int_0^{\tau^+} h_4(\tau)i(t,\tau,\rho)\,d\tau + \sigma_Q\overline{q}(t,\rho), q^*(t,\rho)\Big\rangle_{Y_1} = 0,\\
&\Big\langle \overline{q}(t,\rho), -\Big(\frac{\partial q^*(t,\rho)}{\partial t} + d_Q\Delta q^*(t,\rho) - \sigma_Q q^*(t,\rho)\Big)\Big\rangle_{Y_1}\\
&- \int_0^T\int_\Omega \Big(\int_0^{\tau^+} q_I(\tau)\overline{i}(t,\tau,\rho)\,d\tau\Big)q^*(t,\rho)d\rho dt\\
&- \int_0^T\int_\Omega \Big(\int_0^{\tau^+} h_4(\tau)i(t,\tau,\rho)\,d\tau\Big)q^*(t,\rho)d\rho dt = 0.
\end{aligned}
\tag{5.13}
$$

$$
\begin{aligned}
&\Big\langle \Big(\frac{\partial}{\partial t} - d_R\Delta + v_R(t) + \delta\Big)\overline{r}(t,\rho) - \int_0^{\tau^+} \sigma_I(\tau)\overline{i}(t,\tau,\rho)\,d\tau - \sigma_Q\overline{q}(t,\rho) + h_3(t)r(t,\rho), r^*(t,\rho)\Big\rangle_{Y_1} = 0,\\
&\Big\langle \overline{r}(t,\rho), -\Big(\frac{\partial r^*(t,\rho)}{\partial t} + d_R\Delta r^*(t,\rho) - (v_R(t)+\delta)r^*(t,\rho)\Big)\Big\rangle_{Y_1}\\
&- \int_0^T\int_\Omega \sigma_Q\overline{q}(t,\rho)r^*(t,\rho)d\rho dt - \int_0^T\int_\Omega \Big(\int_0^{\tau^+} \sigma_I(\tau)\overline{i}(t,\tau,\rho)\,d\tau\Big)r^*(t,\rho)d\rho dt\\
&+ \int_0^T\int_\Omega h_3(t)r(t,\rho)r^*(t,\rho)d\rho dt = 0.
\end{aligned}
\tag{5.14}
$$

$$\Big\langle \frac{\partial \overline{v}(t,\rho)}{\partial t} - d_V \Delta \overline{v}(t,\rho) - v_S(t)\overline{s}(t,\rho) - h_2(t)s(t,\rho) - v_R(t)\overline{r}(t,\rho) - h_3(t)r(t,\rho), v^*(t,\rho)\Big\rangle_{Y_1} = 0,$$

$$\begin{aligned}
&\Big\langle \overline{v}(t,\rho), -\Big(\frac{\partial v^*(t,\rho)}{\partial t} + d_V \Delta v^*(t,\rho)\Big)\Big\rangle_{Y_1} \\
&- \int_0^T \int_\Omega \Big(v_S(t)\overline{s}(t,\rho) + v_R(t)\overline{r}(t,\rho)\Big)v^*(t,\rho)d\rho dt \\
&- \int_0^T \int_\Omega \Big(h_2(t)s(t,\rho) + h_3(t)r(t,\rho)\Big)v^*(t,\rho)d\rho dt = 0.
\end{aligned} \tag{5.15}$$

From these equations, the adjoint system corresponding to the control system (5.1) is

$$\begin{aligned}
\frac{\partial s^*(t,\rho)}{\partial t} &= -d_S \Delta s^*(t,\rho) + v_S(t)(s^*(t,\rho) - v^*(t,\rho)) + a(t)s^*(t,\rho)\int_0^{\tau^+} b(\tau)i(t,\tau,\rho)\,d\tau, \\
\frac{\partial i^*(t,\tau,\rho)}{\partial \tau} + \frac{\partial i^*(t,\tau,\rho)}{\partial t} &= -d_I \Delta i^*(t,\tau,\rho) + m(\tau)i^*(t,\tau,\rho) + a(t)b(\tau)s(t,\rho)s^*(t,\rho) \\
&\quad - q_I(\tau)q^*(t,\rho) - \sigma_I(\tau)r^*(t,\rho) + A_1, \\
\frac{\partial q^*(t,\rho)}{\partial t} &= -d_Q \Delta q^*(t,\rho) + \sigma_Q(q^*(t,\rho) - r^*(t,\rho)), \\
\frac{\partial r^*(t,\rho)}{\partial t} &= -d_R \Delta r^*(t,\rho) + v_R(t)(r^*(t,\rho) - v^*(t,\rho)) + \delta(r^*(t,\rho) - s^*(t,\rho)), \\
\frac{\partial v^*(t,\rho)}{\partial t} &= -d_V \Delta v^*(t,\rho), \\
\frac{\partial s^*(t,\rho)}{\partial n} = \frac{\partial i^*(t,\tau,\rho)}{\partial n} &= \frac{\partial q^*(t,\rho)}{\partial n} = \frac{\partial r^*(t,\rho)}{\partial n} = \frac{\partial v^*(t,\rho)}{\partial n} = 0, \quad \rho \in \mathbb{R}^N \setminus \Omega.
\end{aligned} \tag{5.16}$$

The corresponding transversality conditions are:

$$s^*(T,\cdot) = i^*(T,\cdot,\cdot) = q^*(T,\cdot) = r^*(T,\cdot) = v^*(T,\cdot) = i^*(\cdot,\tau^+,\cdot) = 0. \tag{5.17}$$

We are now in a position to prove the existence of an optimal control for system (5.1).

5.3. **Existence and characterization of the optimal control.** This subsection demonstrates the existence of an optimal control and provides its explicit characterization. We define

$$F(a, v_S, v_R, q_I) = \begin{cases} \mathcal{F}(a, v_S, v_R, q_I): & \text{if } (a, v_S, v_R, q_I) \in \mathcal{U}, \\ \infty & \text{otherwise.} \end{cases} \tag{5.18}$$

The existence of an optimal control is established by the following theorem.

Theorem 5.11. *The control problem* (5.1)*, admits a solution* $(a^*, v_S^*, v_R^*, q_I^*) \in \mathcal{U}$ *such that*

$$\min_{(a,v_S,v_R,q_I)\in\mathcal{U}} F(a, v_S, v_R, q_I) = F(a^*, v_S^*, v_R^*, q_I^*).$$

This establishes that $(a^*, v_S^*, v_R^*, q_I^*)$ *is the required optimal control that minimizes our objective functional.*

Proof. We let $l = (a, v_S, v_R, q_I) \in \mathcal{U}$. By the definition of $\mathcal{U}$, it follows that the control variables a, v_S, v_R and q_I are uniformly bounded. Hence from [18] these exists a minimizing sequence $l^{(n)} = (a^{(n)}, v_S^{(n)}, v_R^{(n)}, q_I^{(n)})$ such that

$$\lim_{n\to\infty} F(a^{(n)}, v_S^{(n)}, v_R^{(n)}, q_I^{(n)}) = \inf_{(a,v_S,v_R,q_I)\in\mathcal{U}} F(a, v_S, v_R, q_I). \tag{5.19}$$

We define a space $\widetilde{H} = L^\infty([0,T]) \times L^\infty([0,T]) \times L^\infty([0,T]) \times L^\infty(0,\tau^+)$. Since $l^{(n)}$ is a minimizing sequence, we obtain that $a^{(n)}, v_S^{(n)}, v_R^{(n)}$ are uniformly bounded in $L^\infty([0,T])$ and $q_I^{(n)}$ is uniformly bounded in $L^\infty(0,\tau^+)$. Then, from the Banach-Alaoglu theorem, we can extract a subsequence $l^{(n^k)} = (a^{(n^k)}, v_S^{(n^k)}, v_R^{(n^k)}, q_I^{(n^k)})$ such that

$$l^{(n^k)} \to l^* = (a^*, v_S^*, v_R^*, q_I^*) \quad \text{weakly in } \widetilde{H}.$$

Since $\mathcal{U}$ is convex and closed in $\widetilde{H}$, $l^* \in \mathcal{U}$.

Let $w^{(n^k)} = (s^{(n^k)}, i^{(n^k)}, q^{(n^k)}, r^{(n^k)}, v^{(n^k)})$ be the solution of the system (5.1) corresponding to the sequence $l^{(n^k)}$, i.e., $s^{(n^k)} = s(l^{(n^k)})$, $i^{(n^k)} = i(l^{(n^k)})$, $q^{(n^k)} = q(l^{(n^k)})$, $r^{(n^k)} = r(l^{(n^k)})$ and $v^{(n^k)} = v(l^{(n^k)})$. By applying Theorem (5.9) and Arzelà-Ascoli theorem we conclude that $s^{(n^k)}, i^{(n^k)}, q^{(n^k)}, r^{(n^k)}$ and $v^{(n^k)}$ are continuous, uniformly bounded and relatively compact. Hence there exists a subsequence $w^{(n^{k^r})}$ of $w^{(n^k)}$ such that $w^{(n^{k^r})} \to w^* = (s_*, i_*, q_*, r_*, v_*)$. By continuity of state variables, we obtain $s_* = s(l^*)$, $i_* = i(l^*)$, $q_* = q(l^*)$, $r_* = r(l^*)$ and $v_* = v(l^*)$. We relabel the subsequence $w^{(n^{k^r})}$ by $w^{(m)} = (a^{(m)}, v_S^{(m)}, v_R^{(m)}, q_I^{(m)})$ for ease of notation. Using lower semi-continuity of a^2, v_S^2, v_R^2 and q_I^2, we have

$$\begin{aligned}
&\int_0^T (v_S^*(t))^2 dt \le \liminf_{m\to\infty} \int_0^T (v_S^{(m)}(t))^2 dt, \quad \int_0^T (v_R^*(t))^2 dt \le \liminf_{m\to\infty} \int_0^T (v_R^{(m)}(t))^2 dt,\\
&\int_0^T (a^*(t))^2 dt \le \liminf_{m\to\infty} \int_0^T (a^{(m)}(t))^2 dt, \quad \int_0^{\tau^+} (q_I^*(t))^2 dt \le \liminf_{m\to\infty} \int_0^{\tau^+} (q_I^{(m)}(t))^2 dt.
\end{aligned} \tag{5.20}$$

Similarly, relabel $i^{(n^{k^r})}$ by $i^{(m)}$, then we have

$$\begin{aligned}
&F(a^*, v_S^*, v_R^*, q_I^*)\\
&= \int_0^T \int_0^{\tau^+} \int_\Omega A_1 i_*(t,\tau,\rho)\, d\rho\, d\tau\, dt + \int_0^{\tau^+} \frac{1}{2} A_5 (q_I^*(\tau))^2 d\tau\\
&\quad + \int_0^T \frac{1}{2}\Big(A_2 (v_S^*(t))^2 + A_4 (a^*(t))^2 + A_3 (v_R^*(t))^2\Big) dt\\
&\le \liminf_{m\to\infty} \int_0^T \int_0^{\tau^+} \int_\Omega A_1 i^{(m)}(t,\tau,\rho)\, d\rho\, d\tau\, dt + \int_0^T \frac{1}{2}\Big(A_2 (v_S^{(m)}(t))^2 + A_3 (v_R^{(m)}(t))^2\Big) dt\\
&\quad + \int_0^T \frac{1}{2} A_4 (a^{(m)}(t))^2 dt + \int_0^{\tau^+} \frac{1}{2} A_5 (q_I^{(m)}(\tau))^2 d\tau\\
&= \lim_{m\to\infty} F(a^{(m)}, v_S^{(m)}, v_R^{(m)}, q_I^{(m)})\\
&= \inf_{(a, v_S, v_R, q_I)\in\mathcal{U}} F(a, v_S, v_R, q_I).
\end{aligned} \tag{5.21}$$

Thus $F(l^*) \le \inf_{l\in\mathcal{U}} F(l)$ and hence, l^* is the optimal control that optimizes the objective function $\mathcal{F}$. □

Next, we present and prove a result that characterizes the optimal control explicitly.

Theorem 5.12. *Let (s, e, q, r, v) and $(s^*, e^*, q^*, r^*, v^*)$ be the solution of systems (5.1) and (5.16), respectively. If $l^* = (a^*, v_S^*, v_R^*, q_I^*)$ is the optimal control that minimizes the objective function $\mathcal{F}$, then*

$$\begin{aligned}
a^*(t) &= \max\Big\{0, \min\Big\{a^M, \frac{\int_\Omega \Big(\int_{\tau^+}^0 b(\tau) i(t,\tau,\rho)\, d\tau\Big) s(t,\rho) s^*(t,\rho) d\rho}{A_4}\Big\}\Big\},\\
v_S^*(t) &= \max\Big\{0, \min\Big\{v_S^M, \frac{\int_\Omega s(t,\rho)\Big(v^*(t,\rho) - s^*(t,\rho)\Big) d\rho}{A_2}\Big\}\Big\},\\
v_R^*(t) &= \max\Big\{0, \min\Big\{v_R^M, \frac{\int_\Omega r(t,\rho)\Big(v^*(t,\rho) - r^*(t,\rho)\Big) d\rho}{A_3}\Big\}\Big\},\\
q_I^*(\tau) &= \max\Big\{0, \min\Big\{q_I^M, \frac{\int_0^T \int_\Omega i(t,\tau,\rho)\Big[q^*(t,\rho) - i^*(t,\tau,\rho)\Big] d\rho dt}{A_5}\Big\}\Big\}.
\end{aligned} \tag{5.22}$$

Proof. We have

$$\mathcal{F}'(a,v_S,v_R,q_I)=\int_0^T\int_0^{\tau^+}\int_\Omega A_1\bar{i}(t,\tau,\rho)\,d\rho\,d\tau\,dt+\int_0^T\Big(A_2v_S(t)h_2(t)+A_3v_R(t)h_3(t)+A_4a(t)h_1(t)\Big)dt+\int_0^{\tau^+}A_5q_I(\tau)h_4(\tau)\,d\tau.$$

Using the adjoint system (5.16), we obtain the expression

$$\begin{aligned}
&\int_0^T\int_0^{\tau^+}\int_\Omega A_1\bar{i}(t,\tau,\rho)\,d\rho\,d\tau\,dt\\
&=\int_0^T\int_0^{\tau^+}\int_\Omega \bar{i}(t,\tau,\rho)\Big[\frac{\partial i^*(t,\tau,\rho)}{\partial\tau}+\frac{\partial i^*(t,\tau,\rho)}{\partial t}+d_I\Delta i^*(t,\tau,\rho)\\
&\quad-m(\tau)i^*(t,\tau,\rho)-a(t)b(\tau)s(t,\rho)s^*(t,\rho)+q_I(\tau)q^*(t,\rho)+\sigma_I(\tau)r^*(t,\rho)\Big]\,d\rho\,d\tau\,dt\\
&\quad+\int_0^T\int_\Omega\overline{s}(t,\rho)\Big[\frac{\partial s^*(t,\rho)}{\partial t}+d_S\Delta s^*(t,\rho)-a(t)s^*(t,\rho)\int_0^{\tau^+}b(\tau)i(t,\tau,\rho)\,d\tau\\
&\quad-v_S(t)(s^*(t,\rho)-v^*(t,\rho))\Big]d\rho dt+\int_0^T\int_\Omega\overline{q}(t,\rho)\Big[\frac{\partial q^*(t,\rho)}{\partial t}+d_Q\Delta q^*(t,\rho)\\
&\quad-\sigma_Q(q^*(t,\rho)-r^*(t,\rho))\Big]d\rho\,dt+\int_0^T\int_\Omega\overline{r}(t,\rho)\Big[\frac{\partial r^*(t,\rho)}{\partial t}+d_R\Delta r^*(t,\rho)\\
&\quad-v_R(t)(r^*(t,\rho)-v^*(t,\rho))-\delta(r^*(t,\rho)-s^*(t,\rho))\Big]d\rho dt+\int_0^T\int_\Omega\overline{v}(t,\rho)\Big[\frac{\partial v^*(t,\rho)}{\partial t}\\
&\quad+d_V\Delta v^*(t,\rho)\Big]d\rho dt.
\end{aligned}$$

It follows from (5.10)-(5.15) that

$$\begin{aligned}
&\int_0^T\int_0^{\tau^+}\int_\Omega A_1\bar{i}(t,\tau,\rho)\,d\rho\,d\tau\,dt\\
&=\int_0^T\int_\Omega\Big[h_1(t)\Big(\int_0^{\tau^+}b(\tau)i(t,\tau,\rho)\,d\tau\Big)s(t,\rho)s^*(t,\rho)\Big]d\rho dt\\
&\quad+\int_0^T\int_\Omega h_2(t)s(t,\rho)\Big[s^*(t,\rho)-v^*(t,\rho)\Big]d\rho dt\\
&\quad+\int_0^T\int_\Omega h_3(t)r(t,\rho)\Big[r^*(t,\rho)-v^*(t,\rho)\Big]d\rho dt\\
&\quad+\int_0^T\int_0^{\tau^+}\int_\Omega h_4(\tau)i(t,\tau,\rho)\Big[i^*(t,\tau,\rho)-q^*(t,\rho)\Big]\,d\rho\,d\tau\,dt.
\end{aligned}\tag{5.23}$$

Putting (5.23) in the derivative of $\mathcal{F}$ we obtain

$$\begin{aligned}
\mathcal{F}'(a,v_S,v_R,q_I)&=\int_0^T h_1(t)\Big[\int_\Omega\Big(\int_0^{\tau^+}b(\tau)i(t,\tau,\rho)\,d\tau\Big)s(t,\rho)s^*(t,\rho)d\rho+A_4a(t)\Big]dt\\
&\quad+\int_0^T h_2(t)\Big[\int_\Omega s(t,\rho)\Big(s^*(t,\rho)-v^*(t,\rho)\Big)d\rho+A_2v_S(t)\Big]dt\\
&\quad+\int_0^T h_3(t)\Big[\int_\Omega r(t,\rho)\Big(r^*(t,\rho)-v^*(t,\rho)\Big)d\rho+A_3v_R(t)\Big]dt\\
&\quad+\int_0^{\tau^+}h_4(\tau)\Big[\int_0^T\int_\Omega i(t,\tau,\rho)\Big[i^*(t,\tau,\rho)-q^*(t,\rho)\Big]d\rho dt+A_5q_I(\tau)\Big]d\tau.
\end{aligned}$$

Since $l^* = (a^*, v_S^*, v_R^*, q_I^*)$ minimizes the objective functional $\mathcal{F}$, it follows that $\mathcal{F}'(a^*, v_S^*, v_R^*, q_I^*) \geq 0$. Finally, by incorporating the control constraints specified in (5.3), we obtain the control variables specified in (5.22). □

The structure of the optimal controls in (5.22) reveals how intervention efforts respond to the epidemic dynamics. The social distancing control $a(t)$ is driven by the spatially aggregated infection pressure, weighted by the susceptible population and the corresponding adjoint variable, implying that distancing is intensified when reducing transmission yields a larger marginal benefit relative to its cost. The vaccination controls $v_S(t)$ and $v_R(t)$, which depend on the difference between the adjoint variables of the vaccinated and unvaccinated compartments, weighted by the sizes of the susceptible and recovered populations, respectively. This indicates that vaccination effort is increased when transferring individuals into the vaccinated class produces a greater epidemiological gain relative to vaccination cost.

The optimal quarantine strategy $q(\tau)$ is determined by the cumulative contribution of infected individuals at infection age τ to the objective functional, weighted by the corresponding adjoint variables. Consequently, infection stages that contribute more strongly to transmission or incur higher epidemiological cost are assigned higher quarantine intensity, rather than applying isolation uniformly across all stages of infection.

6. Numerical simulation

To explore the behavior of our model and demonstrate the numerical solution of the associated optimal control problem, we carried out numerical simulations using biologically realistic parameter values, chosen to reflect the transmission dynamics of measles. The analysis is divided into three main parts: (i) Examining disease persistence and elimination under different threshold conditions, (ii) exploring the impact of infected individual mobility on spatial spread, and (iii) assessing the role and evolution of time-dependent control strategies.

For the uncontrolled case, we applied an explicit finite difference scheme to solve the state system (2.1). For the optimal control problem, we employed the well-established forward-backward sweep method. This approach begins with an initial guess for the control variables. We then solve the state equations (5.1) forward in time, followed by backward integration of the adjoint system (5.16) using the computed state solutions. Finally, the control variables are updated based on these solutions. This process is repeated until successive control approximations converge to within a specified tolerance. Further details on the forward-backward sweep method can be found in [18].

The time domain, spatial domain, and infection-age domain are considered as $[0, T] = [0, 100]$, $\Omega = [0, L] = [0, 10]$, and $[0, \tau^+] = [0, 28]$, respectively. The initial state of the model is taken as

$$\begin{aligned} S_0(\rho) &= 0.9 + 0.05 \sin\Big(\frac{\pi\rho}{L}\Big), \quad I_0(\tau, \rho) = 0.01e^{-0.5\tau} + 0.05 \sin\Big(\frac{\pi\rho}{L}\Big), \\ Q_0(\rho) &= 0.01e^{-(\rho - \frac{L}{2})^2}, \quad R_0(\rho) = 0.01 \cos\Big(\frac{\pi\rho}{2L}\Big)^2, \quad R_0(\rho) = 0.02 \sin\Big(\frac{\pi\rho}{L}\Big)^2. \end{aligned} \tag{6.1}$$

To keep the model computationally manageable and also since there is no strong biological evidence suggesting significant differences in the spatial movement of various population groups during measles transmission, we use the same diffusion rate d_1 for all compartments. This simplification enables us to focus more effectively on the age structure of infections and the role of control strategies. Based on Assumptions 2.2 and 2.3, along with available epidemiological data on measles, we have chosen the parameter values listed in Table 1.

The infection-age dependent transmission rate is taken as $\beta(\tau) = 2e^{-(\tau-10)^2/8}$, $q_I(\tau) = 0.2e^{-0.2\tau}$. Mortality rate due to infection is taken as $d(\tau) = 0.001e^{-0.05\tau}$. The recovery rate of infected individuals is taken as $\sigma_I(\tau) = \frac{1}{14} \cdot \chi_{[14,21]}(\tau)$, where

$$\chi_{[14,21]}(\tau) = \begin{cases} 1 & \text{if } \tau \in [14, 21], \\ 0 & \text{otherwise.} \end{cases}$$

Also, we define total infected population at time t and location ρ by $I_{\text{tot}}(t, \rho) = \int_0^{\tau^+} I(t, \tau, \rho)\, d\tau$.

TABLE 1. Model parameters, units, and values used in simulations.

Symbol	Units	Value(Case 1/Case 2)
A	individuals/day	0.005/0.05
μ	day^{-1}	0.02/0.005
v_S	day^{-1}	0.2/0.02
v_R	day^{-1}	0.05
δ	day^{-1}	0.05
σ_Q	day^{-1}	0.1
d_1	km^2/day	0.1
T	days	100
τ^+	days	28
L	km	10

6.1. **Influence of $\mathcal{R}_0$ on Disease dynamics.** Figure 1 shows the temporal dynamics of the compartments S, I_{tot}, Q, R and V at the location $\rho = 4.898$. From Remark 4.3 regarding the $\mathcal{R}_0$, we have two cases:

Case 1 (Sub-threshold). With mortality rate $\mu = 0.02$, vaccination rate $v_S = 0.2$ and recruitment rate $A = 0.005$, we obtain $\mathcal{R}_0 = 0.32859 < 1$. Figure 1(a) depicts this scenario, where the infection fails to sustain itself and quickly dies out. The susceptible population declines slightly before stabilizing, while the infected, quarantined, and recovered classes decay to near-zero levels. The vaccinated population initially increases due to the strong vaccination rate and later stabilizes as disease transmission ceases. This behavior is consistent with theoretical expectations for sub-threshold dynamics.

Case 2 (Super-threshold). When the recruitment rate is increased to $A = 0.05$, the mortality reduced to $\mu = 0.005$, and the vaccination rate lowered to $v_S = 0.02$, the basic reproduction number rises to $\mathcal{R}_0 = 37.5049 > 1$. Figure 1(b) illustrates this case, where the infection persists over time, with the infected population showing oscillatory behavior instead of dying out. All compartments demonstrate sustained temporal dynamics: susceptibles fluctuate, indicating recurrent infection waves; quarantined and recovered individuals also oscillate due to ongoing transmission and control interactions. The vaccinated population steadily increases as vaccination continues, though not enough to bring $\mathcal{R}_0$ below 1. These dynamics confirm that the disease becomes endemic in the population.

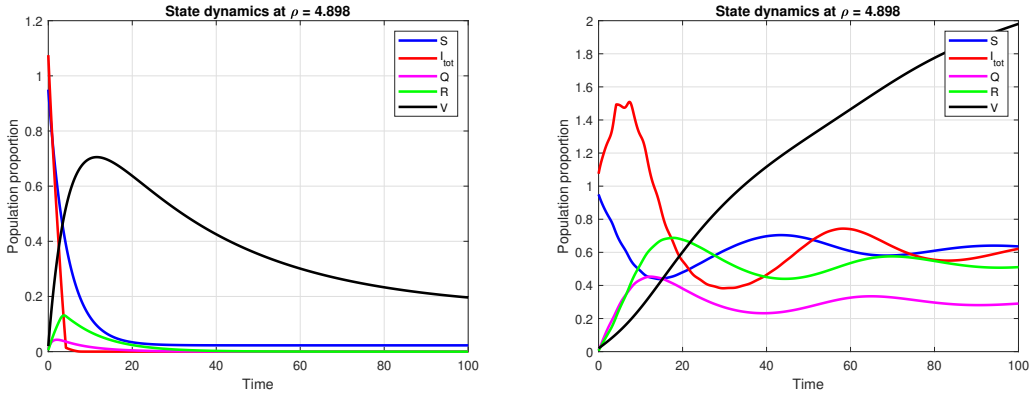

(a) Case 1: $\mathcal{R}_0 < 1$ (b) Case 2: $\mathcal{R}_0 > 1$

FIGURE 1. Temporal dynamics of all state variables at $\rho = 4.898$.

6.2. **Impact of infected population mobility on spatiotemporal spread of infection.** To examine how the mobility of infected individuals influences spatial transmission, we simulate the

model under two diffusion rates for the infected class: $d_I = 0.01$ and $d_I = 0.5$. Other parameters are fixed as in Case 2 (i.e., $\mathcal{R}_0 > 1$). Figure 2 illustrates the resulting spatiotemporal dynamics of the total infected population $I_{\text{tot}}(t, \rho)$.

In Figure 2(a) for low mobility ($d_I = 0.01$), the infection remains spatially localized and displays sharp peaks over space, indicating limited spread. The outbreak is concentrated around regions of initial infection, and the spatial heterogeneity is more pronounced. This reflects minimal mixing of infected individuals across the domain.

In contrast, Figure 2(b), corresponding to high mobility ($d_I = 0.5$), shows a smoother, more widespread infection profile. The infected individuals diffuse more uniformly across space, causing the disease burden to distribute more evenly. Although the spatial peaks are less sharp, the infection persists for longer durations across the domain due to greater mixing and seeding of new regions.

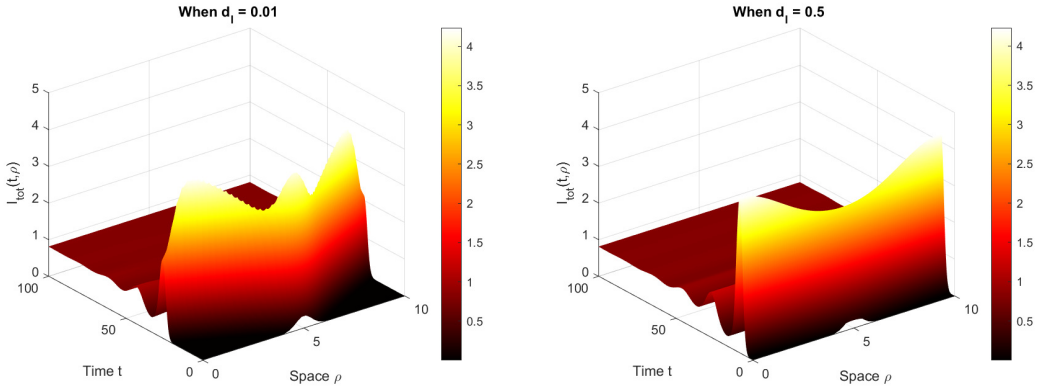

(a) Case 1: $d_I = 0.01$ (b) Case 2: $d_I = 0.5$.

FIGURE 2. Effect of diffusion coefficient d_I on the spatiotemporal spread of infection.

Remark 6.1. These findings underscore the critical role of infected population mobility in shaping the spatiotemporal dynamics of disease transmission. Higher diffusion rates facilitate broader and more persistent spatial spread, enabling the infection to sustain itself even when localized outbreaks subside. This insight is valuable for designing spatially targeted interventions, such as regional lockdowns or mobility restrictions, and for anticipating potential hotspots or secondary waves of infection.

6.3. **Evolution of optimal control variables.** Figure 3 illustrates the evolution of the optimal control variables over time and infection age. The upper bounds for all controls are uniformly set as $a^M = v_S^M = v_R^M = q_I^M = 1$. Also, we chose the objective weights to be $A_1 = A_2 = A_3 = A_4 = 1$ and $A_5 = 0.1$. Other parameters are also chosen as per Case 2 (i.e., $\mathcal{R}_0 > 1$).

Remark 6.2. To reflect the biological effectiveness of stage-specific interventions, we assign a lower weight to the infection-age dependent control $q_I(\tau)$ by choosing a small value for A_5. Assigning a lower value to A_5 makes the model more inclined to apply stronger isolation measures based on infection age, especially during periods of high infectivity (e.g., rash phase in measles, which lasts between 14-21 days). Biologically, this means focusing efforts on isolating individuals when they are most contagious, rather than applying broad, costly interventions. This targeted strategy helps in reducing transmission efficiently while controlling overall costs.

Figure 3(a) represents the trajectory of the control function $a(t)$, which modulates the effective contact rate. The curve initially dips, followed by a rise around the middle of the simulation horizon, and gradually decreases thereafter. This non-monotonic behavior suggests that moderate efforts to reduce transmission should begin early and be intensified during the critical phase of infection spread, followed by a less aggressive strategy once the disease burden diminishes.

Figure 3(b) displays the vaccination rate of susceptible, $v_S(t)$. The curve starts at a higher value, indicating an early push to vaccinate the susceptible population to curb transmission. As time progresses, the rate declines steadily, reflecting that most susceptible individuals are either vaccinated or have exited the susceptible class due to infection or other transitions. The decay in the curve is smooth, suggesting a sustained but diminishing effort as the population's susceptibility diminishes.

Figure 3(c) shows the control $v_R(t)$, the vaccination rate for recovered individuals, possibly due to waning immunity or incomplete natural immunity. The curve remains low throughout the simulation but shows a small peak in the early phase. The relatively small magnitude of $v_R(t)$ reflects that post-recovery vaccination is not a dominant intervention in the optimal strategy, either due to the low risk of reinfection or lower cost-effectiveness compared to other controls. The optimal strategy favors vaccinating recovered individuals primarily in the intermediate phase of the epidemic when their population is substantial.

Figure 3(d) depicts the infection-age dependent quarantine control $q_I(\tau)$. This function varies with infection age and exhibits peaks during the mid-age of infection, particularly between days 10 and 20, which is aligned with the period of highest infectivity. This targeted approach highlights the value of age-dependent interventions that concentrate resources during the most critical window of transmission.

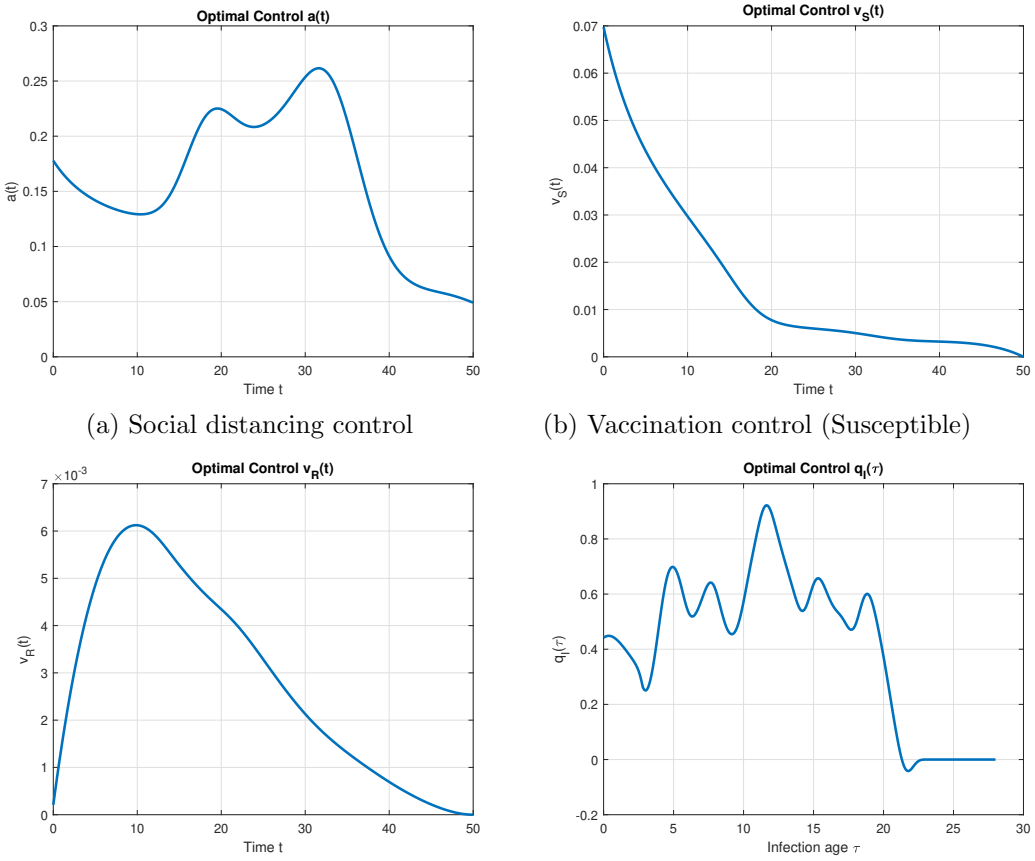

(a) Social distancing control

(b) Vaccination control (Susceptible)

(c) Vaccination control (Recovered)

(d) Quarantine control

FIGURE 3. Dynamics of control variables.

7. Discussions and concluding remarks

Infectious disease dynamics are often influenced not just by who is infected, but by how long individuals have been infected. The notion of infection age offers a crucial structural variable

for modeling the progression of disease, capturing changes in infectiousness, symptom severity, and responsiveness to interventions over time. In this study, we proposed a novel infection-age structured reaction-diffusion model to examine the spatiotemporal spread of disease under the combined influence of vaccination, quarantine, and recovery-driven mechanisms. Our goal was to explore how the timing and nature of interventions, such as contact reduction, targeted vaccination, and stage-specific isolation, shape the overall epidemic trajectory when infectivity varies throughout the course of infection.

Through the threshold analysis, we derived the basic reproduction number $\mathcal{R}_0$, which governs whether the disease will persist or die out. The structure of $\mathcal{R}_0$ reveals its sensitivity to the recruitment rate of susceptible individuals and the extent of vaccination coverage. Since our model incorporates realistic assumptions and captures essential features of disease spread, it offers valuable insight for policymakers. In particular, it can help design vaccination campaigns that are both cost-effective and epidemiologically sufficient, enabling optimal use of public health resources without unnecessary overspending.

Building on this threshold-based understanding, our optimal control analysis further highlights how carefully timed and targeted interventions can suppress disease transmission without incurring high costs. The structure of the optimal controls in our model reveals how intervention strategies adapt dynamically based on the interaction between state and adjoint variables. The control $a^*(t)$, tied to contact reduction, is most active when both susceptibility and infection levels are high, reflecting its maximal impact during peak transmission. The vaccination controls $v_S^*(t)$ and $v_R^*(t)$ are guided by the gap between adjoint and state variables, prioritizing vaccination when it yields the greatest marginal benefit. Meanwhile, the infection-age dependent quarantine $q_I^*(\tau)$ targets the period of peak infectiousness, ensuring isolation is applied when most effective. These structure-driven strategies allow for more efficient resource allocation, directing control efforts to where they are most needed.

To demonstrate the applicability of our model, we simulated its behavior under parameter values suitable for measles, a well-studied disease with strong infection- age dynamics. Our results showed that early and aggressive contact reduction and susceptible vaccination are vital for outbreak control. Among all interventions, the infection-age dependent quarantine proved especially effective during the peak infectious window (days 10-20), aligning with the known epidemiology of measles. These findings reinforce the importance of age-targeted public health responses and support real-world strategies that focus on isolating high-risk individuals rather than implementing broad, costly interventions.

Overall, this study emphasizes the significance of infection age, spatial diffusion, and targeted control in managing infectious diseases. While our model captures key features of infection progression and spatial transmission, it remains idealized in several respects. It does not account for host heterogeneity, behavioral adaptation, or stochastic variation. Moreover, parameter estimation is limited by the availability of infection-age-structured data in real-world settings. Future extensions may involve time-varying diffusion, demographic heterogeneity, and data-driven calibration, which would enhance both the predictive power and the applicability of the model in public health planning.

Acknowledgments. The authors want to thank the anonymous reviewers for their valuable comments that improved the quality of the manuscript.

References

[1] L. J. Allen, B. M. Bolker, Y. Lou, A. L. Nevai; *Asymptotic profiles of the steady states for an SIS epidemic reaction-diffusion model*, Discrete Contin. Dyn. Syst. 21(1) (2008), 1-20.

[2] H. Amann; *Fixed point equations and nonlinear eigenvalue problems in ordered Banach spaces*, SIAM Rev. 18 (1976), 620-709.

[3] V. Barbu; *Mathematical Methods in Optimization of Differential Systems*, Kluwer Academic, Dordrecht, 1994.

[4] R. S. Cantrell, C. Cosner; *Spatial Ecology Via Reaction-Diffusion Equations*, in: Mathematical and Computational Biology, John Wiley Sons Ltd., West Sussex, England, 2003.

[5] N. Chanauria, S. Abbas; *Stability analysis of an age-structured SIR model with nonlocal diffusion and indirect contacts*, Discrete Contin. Dyn. Syst. Ser. B 29(6) (2024), 2532-2548.

[6] P. Colli, G. Gilardi, G. Marinoschi, E. Rocca; *Optimal control of a reaction-diffusion model related to the spread of COVID-19*, Anal. and Appl. 22 (2024), 111-136.
[7] O. Diekmann, J. A. P. Heesterbeek, J .A. J. Metz; *On the definition and the computation of the basic reproduction ratio R_0 in models for infectious diseases in heterogeneous populations*, J. Math. Biol. 28 (1990), 365-382.
[8] K. R. Fister, S. Lenhart; *Optimal control of a competitive system with age structure*, J. Math. Anal. Appl. 291 (2) (2004), 526-537.
[9] H. Hethcote; *The mathematics of infectious diseases*, SIAM Rev. 42(4) (2000), 599-653.
[10] S. B. Hsu, F. B. Wang, X. Q. Zhao; *Dynamics of a periodically pulsed bio-reactor model with a hydraulic storage zone*, J. Dynam. Differential Equations 23 (2011), 817-842.
[11] H. Inaba; *Age-Structured Population Dynamics in Demography and Epidemiology*. Springer 2017.
[12] O. R. Isik, N. Tuncer, M. Martcheva; *A mathematical model for the role of vaccination and treatment in measles transmission in Turkey*, J. Comput. Appl. Math. 457 (2025), 116308.
[13] J. Jang, H. Kwon, J. Lee; *Optimal control problem of an SIR reaction-diffusion model with inequality constraints*, Math. Comput. Simulation 171 (2020), 136-151.
[14] Z. Jiao, I. Jadlovská, T. Li; *Analysis of an SIS reaction-diffusion chemotaxis epidemic model with gradient-dependent flux limitation and standard incidence*, Discrete Contin. Dyn. Syst. Ser. B 29 (2024), no. 9, 3731-3743.
[15] S. Kanchanarat, K. Nudee, S. Chinviriyasit, W. Chinviriyasit; *Mathematical analysis of pulse vaccination in controlling the dynamics of measles transmission*, Infect. Dis. Model. 8(4) (2023), 964-979.
[16] W. Kermack, A. McKendrick; *A contribution to the mathematical theory of epidemics*, Proc. Roy. Soc. London Ser. A 115(772) (1927), 700-721.
[17] C. Lei, H. Li, Y. Zhao; *Dynamical behavior of a reaction-diffusion SEIR epidemic model with mass action infection mechanism in a heterogeneous environment*, Discrete Contin. Dyn. Syst. Ser. B 29(7) (2024), 3163-3198.
[18] S. Lenhart, J. T. Workman; *Optimal Control Applied to Biological Models*, 1st ed., Chapman and Hall/CRC, 2007.
[19] T. Li, D. Acosta-Soba, A. Columbu, G. Viglialoro; *Dissipative Gradient Nonlinearities Prevent δ-Formations in Local and Nonlocal Attraction-Repulsion Chemotaxis Models*, Stud. Appl. Math. 154(2) (2025), e70018.
[20] S. Ma, T. Tian, H. Huo; *Global stability and optimal control of an age-structured SVEIR epidemic model with waning immunity and relapses*, J. Math. Biol. 89(32), (2024).
[21] I. M. Mackay; *Measles: virus, symptoms and white blood cells*, Virology Down Under. Available at: https://virologydownunder.com/measles-and-you-virus-symptoms-and-white-blood-cells/
[22] P. Magal, S. Ruan; *Structured Population Models in Biology and Epidemiology*, Springer 2007.
[23] L. Meng, W. Zhu; *Analysis of SEIR epidemic patch model with nonlinear incidence rate, vaccination and quarantine strategies*, Math. Comput. Simulation 200 (2022), 489-503.
[24] W. J. Moss; *Measles*, Lancet 390 (10111) (2017), 2490-2502.
[25] J. D. Murray; *Mathematical Biology I: An Introduction* (3rd ed.), Springer 2002.
[26] G. Sun, H. Zhang, L. Chang, Z. Jin, H. Wang, S. Ruan; *On the Dynamics of a Diffusive Foot-and-Mouth Disease Model with Nonlocal Infections*, SIAM J. Appl. Math. 82 (2022), 1587-1610.
[27] C. Walker; *Stability and Instability of Equilibria in Age-Structured Diffusive Populations*, J. Dyn. Diff. Equat. 37 (2025), 1315-1354.
[28] P. Wu, H. Zhao; *Mathematical analysis of an age-structured HIV/AIDS epidemic model with HAART and spatial diffusion*, Nonlinear Anal. Real World Appl. 60 (2021), 103289.
[29] T. Wu, Y. Su, X. Zhuo; *Global dynamics of a general degenerate multiscale age-structured HCV diffusive model with spatial heterogeneity*, Discrete Contin. Dyn. Syst. Ser. B 30(8) (2025), 2822-2847.
[30] X. Wu, R. Yuan, F. Chen; *Analysis on mixed types of waves for an SIR epidemic model with infection-age structure and spatial diffusion*, Commun. Nonlinear Sci. Numer. Simul. 149 (2025), 108928.
[31] L. Ye, H. Zhao, X. Zhang, D. Wu; *Complex dynamics of a memory-induced stage-structured diffusive system with maturation delay and strong Allee effect*, Math. Methods Appl. Sci. 48(5) (2025), 6191-6207.
[32] L. Zhao; *Spreading speed and traveling wave solutions of a reaction-diffusion Zika model with constant recruitment*, Nonlinear Anal. Real World Appl. 74(2023), 103942.
[33] Q. Zhao, B. Liu, G. Ren; *Optimal control and dynamics of a nonlocal diffusion SVIR epidemic model*, Math. Control Relat. Fields 15(2) (2025), 809-834.

Nikhil Chanauria
School of Mathematical and Statistical Sciences, Indian Institute of Technology Mandi, Mandi, H.P., 175005, India
Email address: kumar.nikhil437@gmail.com

Syed Abbas
School of Mathematical and Statistical Sciences, Indian Institute of Technology Mandi, Mandi, H.P., 175005, India
Email address: abbas@iitmandi.ac.in, sabbas.iitk@gmail.com